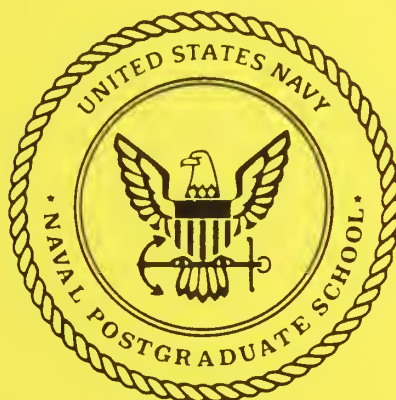


# NAVAL POSTGRADUATE SCHOOL

## Monterey, California



### RECENT ADVANCES IN UNDERSTANDING TROPICAL CYCLONE MOTION

Russell L. Elsberry  
Robert F. Abbey, Jr.

September 1991

Interim Report for Period  
October 1990 - September 1991

Approved for Public Release; Distribution Unlimited

Prepared for: Office of Naval Research (Code 1122MM)  
Arlington, WA 22217

FedDocs  
D 208.14/2  
NPS-MR-91-003

308.14/2  
P2-104-71-003

**Naval Postgraduate School  
Monterey, CA 93943-5000**

Rear Admiral R.W. West  
Superintendent

H. Shull  
Provost

This report was prepared for and funded by the Office of Naval Research, Code 1122MM, Arlington, VA., 22217-5000.

Reproduction of all or part of the report is authorized.

This report was prepared by:

UNCLASSIFIED

NAVAL POSTGRADUATE SCHOOL  
MONTEREY CA 93943-5100

SECURITY CLASSIFICATION OF THIS PAGE

## REPORT DOCUMENTATION PAGE

Form Approved  
OMB No 0704-0188

1a REPORT SECURITY CLASSIFICATION UNCLASSIFIED			1b RESTRICTIVE MARKINGS		
2a SECURITY CLASSIFICATION AUTHORITY			3 DISTRIBUTION/AVAILABILITY OF REPORT Approved for public release; distribution unlimited		
2b DECLASSIFICATION/DOWNGRADING SCHEDULE			5 MONITORING ORGANIZATION REPORT NUMBER(S)		
4 PERFORMING ORGANIZATION REPORT NUMBER(S) NPS-MR-91-003			7a NAME OF MONITORING ORGANIZATION Office of Naval Research (Code 1122MM)		
6a NAME OF PERFORMING ORGANIZATION Naval Postgraduate School			7b ADDRESS (City, State, and ZIP Code) Arlington, VA 22217-5000		
6b OFFICE SYMBOL (If applicable) MR			8a NAME OF FUNDING / SPONSORING ORGANIZATION Office of Naval Research		
6c ADDRESS (City, State, and ZIP Code) Monterey, CA 93943-5000			8b OFFICE SYMBOL (If applicable) Code 1122MM		
8c ADDRESS (City, State, and ZIP Code) Arlington, VA 22217-5000			9 PROCUREMENT INSTRUMENT IDENTIFICATION NUMBER N0001491WR24004		
10 SOURCE OF FUNDING NUMBERS			11 TITLE (Include Security Classification) RECENT ADVANCES IN UNDERSTANDING TROPICAL CYCLONE MOTION (U)		
PROGRAM ELEMENT NO 0601153N			PROJECT NO RR033- 03-0B		
TASK NO			WORK UNIT ACCESSION NO		
12 PERSONAL AUTHOR(S) Russell L. Elsberry and Robert J. Abbey, Jr.					
13a. TYPE OF REPORT Interim		13b TIME COVERED FROM 10/90 to 10/91		14 DATE OF REPORT (Year, Month, Day) 91 September	
15 PAGE COUNT 92					
16 SUPPLEMENTARY NOTATION THE VIEW EXPRESSED IN THIS REPORT ARE THOSE OF THE AUTHOR AND DO NOT REFLECT THE OFFICIAL POLICY OR POSITION OF THE DEPARTMENT OF DEFENSE					
17 COSATI CODES			18 SUBJECT TERMS (Continue on reverse if necessary and identify by block number)		
FIELD	GROUP	SUB-GROUP			
19 ABSTRACT (Continue on reverse if necessary and identify by block number) Some advances in understanding of tropical cyclone motion that have occurred during the last five years are reviewed. Although the focus is on research in support of the Office of Naval Research Tropical Cyclone Motion Initiative, some other studies (especially from a National Oceanic and Atmospheric Administration initiative) are included. Observational studies have detected a propagation vector, which is the departure of the motion vector from the steering flow (defined in a variety of ways). Barotropic models have been used to understand: (i) vortex motion in a quiescent environment on a beta-plane; (ii) vortex outer wind structure effects; (iii) environmental relative vorticity and shear effects; and (iv) adjacent synoptic and mesoscale circulation influences. Recent baroclinic models that include idealized structure and vertical shear to full-physics models with real data are also reviewed briefly.					
20 DISTRIBUTION/AVAILABILITY OF ABSTRACT <input checked="" type="checkbox"/> UNCLASSIFIED/UNLIMITED <input type="checkbox"/> SAME AS RPT <input type="checkbox"/> DTIC USERS			21 ABSTRACT SECURITY CLASSIFICATION UNCLASSIFIED		
22a NAME OF RESPONSIBLE INDIVIDUAL Russell L. Elsberry			22b TELEPHONE (Include Area Code) (408) 646-2373		22c OFFICE SYMBOL MR

DD Form 1473, JUN 86

Previous editions are obsolete

SECURITY CLASSIFICATION OF THIS PAGE

S/N 0102-LF-014-6603

UNCLASSIFIED



## Table of Contents

1.	Introduction	2
2.	Observational studies	4
a.	Radial-band average steering	5
b.	Geostrophic steering	10
c.	Cyclone intensity-dependent steering	11
d.	Individual cases	12
e.	Mechanism for cyclone motion	15
f.	Implications from observational studies	17
3.	Beta-induced propagation	22
a.	Self-advection process	22
b.	Uniform-flow region	25
c.	Analytical models	29
d.	Effect of divergence	33
4.	Vortex structure effects	35
a.	Outer wind effect	35
b.	Relative angular momentum relationships	36
c.	Possibility of observational validation	41
5.	Environmental relative vorticity gradient and shear	43
a.	Relative vorticity gradient	43
b.	Linear shear effect	48
c.	Potential vorticity effect due to layer thickness	50
6.	Adjacent synoptic and mesoscale circulations	51
a.	Binary cyclones	51
b.	Mesoscale circulations	55
7.	Implications of barotropic wind studies	58
a.	Wind field decomposition	58
b.	Detectability of gyres from observations	62
c.	Validation of absolute vorticity gradient dependency	66
d.	Initialization of dynamical track prediction models	68
8.	Baroclinic effects	72
a.	Vertical structure models	72
b.	Vertical shear effect	78
c.	Full-physics baroclinic models	81
	REFERENCES	85





## Abstract

Some advances in understanding of tropical cyclone motion that have occurred during the last five years are reviewed. Although the focus is on research in support of the Office of Naval Research Tropical Cyclone Motion Initiative, some other studies (especially from a National Oceanic and Atmospheric Administration initiative) are included.

Observational studies have detected a propagation vector, which is the departure of the motion vector from the steering flow (defined in a variety of ways). Barotropic models have been used to understand: (i) vortex motion in a quiescent environment on a beta-plane; (ii) vortex outer wind structure effects; (iii) environmental relative vorticity and shear effects; and (iv) adjacent synoptic and mesoscale circulation influences. Recent baroclinic models that include idealized structure and vertical shear to full-physics models with real data are also reviewed briefly.

## 1. Introduction

The Office of Naval Research (ONR) Marine Meteorology Program under Dr. R. F. Abbey, Jr., has sponsored a five-year accelerated research initiative on Tropical Cyclone Motion that began on 1 October 1986. From an operational perspective, the need for improved understanding and prediction of tropical cyclone motion was illustrated by poor track forecasts of a large Typhoon Abby (1984). From a scientific perspective, new ideas and understandings also made the timing right for a special initiative on tropical cyclone motion. The three components of the ONR initiative were analytical and numerical modelling studies, analysis of existing data sets and an experimental program. The purpose of this review is to summarize advances in understanding that have been achieved in the first two components of the ONR initiative. Since the Tropical Cyclone Motion (TCM-90) field experiment was completed only recently in August-September 1990, results from that component will be forthcoming. The first part of the review will consider observational studies and the remainder will address analytical and numerical studies. Journal articles since 1986 constitute the prime source material for the review. However, some recent manuscripts not yet published and some preprints from the 19th Conference on Hurricanes and Tropical Meteorology also have been included.

While the ONR program was being organized during 1985, the United States was struck by a large number of hurricanes that heightened interest in these dangerous storms. The National Oceanic and Atmospheric Administration (NOAA) responded with a



new initiative in research and in operational prediction. Although the primary focus of this review is related to the ONR initiative, the fortunate coincidence with the NOAA initiative contributed much to the advances described. Indeed, NOAA personnel contributed ideas and shared preliminary results in a series of ONR planning meetings (Elsberry 1986, 1987a, 1987b, 1988a, 1988b, 1989a, 1989b, 1989c). Permission of the NOAA Hurricane Research Division (HRD) personnel to quote from their unpublished manuscripts is gratefully acknowledged.

## 2. Observational studies

To first order, the tropical cyclone can be considered as a point vortex that is being advected by a large-scale environmental flow (steering concept, or cork-in-a-stream analogy). Track prediction might then be considered to be a problem of accurately observing and predicting the steering flow. However, observational and numerical modeling studies (to be described below) indicate that the tropical cyclone motion can deviate significantly at times from a large-scale environmental flow. Indeed, one of the primary objectives of recent tropical cyclone motion research has been to specify, understand and predict this deviation.

It is emphasized that the magnitude and direction of this departure from a steering concept depends on the definition of the environment of the tropical cyclone. Thus, the various definitions that have arisen in observational studies will be described. Because of the different definitions in each study, it is difficult to compare the departures from steering. Nevertheless, recent observational studies provide evidence about the general characteristics of the departures, which are useful for interpreting the numerical and analytical models of tropical cyclone motion to be discussed in the following sections.

The observational studies also have provided an indication of the mechanisms that lead to tropical cyclone motion. Because these interpretations tend to rely on limited data sets or a particular analysis technique, the results are not conclusive. Consequently, a combined observational-numerical interpretation

is likely to be helpful. Some preliminary observational verifications of the barotropic, analytical and numerical models will be given in Section 7. However, a more conclusive demonstration of the new understandings on tropical cyclone motion will need to await the results of studies based on the Tropical Cyclone Motion (TCM-90) field experiment data set (Elsberry 1990; Elsberry et al. 1990; Harr et al. 1991).

a. Radial-band average steering

The rawinsonde composite studies (e.g., George and Gray 1976; Chan and Gray 1982; Gray 1989) under Professor William Gray have calculated the departures of the storm motion relative to a steering flow defined as radial-band averages of the vertically-integrated wind observations at various distances from the center. Stratifications have been done for a large variety of storm characteristics such as intensity (defined as maximum winds or minimum central pressure) and size, track directions (west-moving, north-moving, east-moving), track displacements (fast, medium, slow), and storm basins.

In general, the storm motion has been found to be to the left of and faster than the steering defined in terms of radial-band averages as defined by Gray's group (Fig. 1). This is true whether the vertical averaging is over the entire depth of the troposphere or only the layer between the boundary layer and the outflow layer (say 850 mb - 300 mb). This definition of steering generally rotates clockwise in the Northern Hemisphere and diminishes in magnitude at larger radii from the center. Thus,

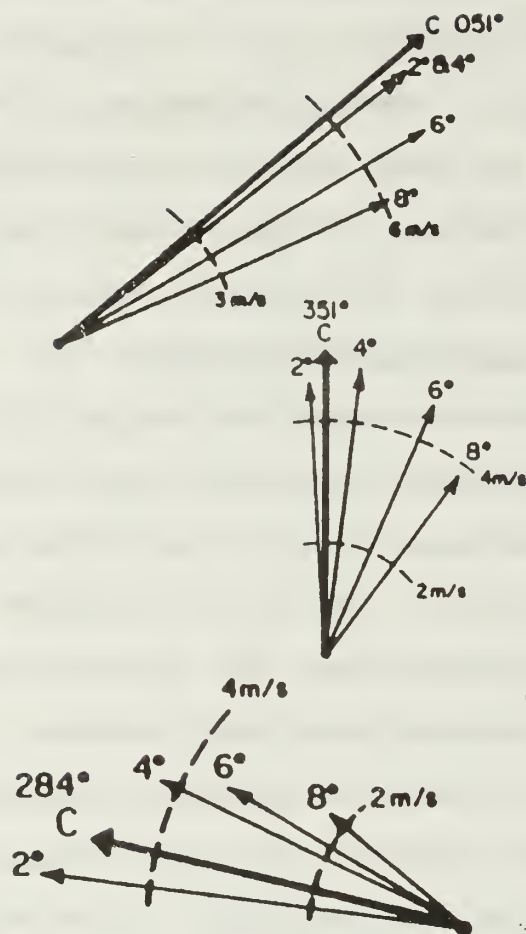


Fig. 1 Layer (850-350 mb) and radial-band ( $2^\circ$  is  $1-3^\circ$  lat.; etc.) average wind vectors relative to the mean cyclone motion (C) for all northeast-moving storms (top), and for moderate translation speed storms moving toward north (middle) or to the west (bottom) from composites of rawinsondes around western North Pacific by Gray (1989). Notice that the radial arcs are 3 and 6  $\text{m s}^{-1}$  in the top panel and 2 and 4  $\text{m s}^{-1}$  in the other two panels.



the departure of the cyclone motion from steering is a function of which radial-band average is selected. A common choice has been the 5-7° lat. radial band (labelled 6° in Fig. 1), so that typical magnitudes of the departures from steering are 1-4 m s<sup>-1</sup>, and the motion is to the left of this steering definition.

Chan (1985) calculated the steering flow in radial-band averages of operationally-analyzed wind fields. Large differences in the flow fields were found among groups of cyclones moving toward the west, the north and the northeast (Table 1). Westward-moving storms had tracks to the right of (7°) and faster than (about 1.5 m s<sup>-1</sup>) the surrounding flow within the 5-7° lat. radial band. Northward-moving cyclones move to the left and faster than the midtropospheric steering flow. Contrasting deviations are found at 700 mb and 400 mb for the northeastward-moving cyclones, with large variability about the mean in a small sample (only 10 cases). Except for the westward-moving storms, the steering-motion relationships from the operationally-analyzed field agree with the rawinsonde composites of Chan and Gray (1982).

Carr and Elsberry (1990) have converted the composite rawinsonde studies of Chan and Gray (1982) and similar composites of Australian cyclones by Holland (1984) to a north-oriented, earth-relative coordinate system. Both studies defined the steering as the radial-band average from 5-7° lat. Holland averaged between 800-300 mb and an average from the surface to 300 mb was used in the Chan and Gray study. Vector differences



**Table 1** Direction (deg.) and speed ( $\text{m s}^{-1}$ ) deviations of the azimuthally-averaged winds within the  $5\text{--}7^\circ$  lat. radial band at 700 mb and 400 mb relative to the mean cyclone motion vector for three stratifications by track direction. A positive number for the direction (speed) deviation means the cyclone is moving to the left of (slower than) the radial-band average definition of the steering (Chan 1985).

<u>Stratification</u>	<u>700 mb</u>		<u>400 mb</u>	
	<u>Direction</u>	<u>Speed</u>	<u>Direction</u>	<u>Speed</u>
Westward ( $265\text{--}285^\circ$ )	-7	-1.7	-1	-1.5
Northward ( $345\text{--}015^\circ$ )	13	-1.7	30	-2.3
Northeastward ( $025\text{--}055^\circ$ )	-25	2.2	27	2.0

**Table 2** Optimum steering levels (mb), correlation coefficients ( $r$ ) between storm motion and calculated geostrophic steering in zonal and meridional directions (in parenthesis), and resultant 24-h forecast error (km) from a dependent sample of  $N$  cases for direction of motion and storm intensity stratifications (Dong and Neumann 1986).

Intensity	N	Optimum Level	r	Error	Optimum Layer	r	Error
WESTWARD-MOVING							
Hurricane	258	400	0.61 (0.67)	180	1000-100	0.60 (0.66)	182
Tropical storm	257	700	0.51 (0.50)	213	1000-400	0.53 (0.51)	213
EASTWARD-MOVING							
Hurricane	191	400	0.78 (0.73)	300	1000-150	0.81 (0.72)	295
Tropical storm	167	700	0.71 (0.58)	293	1000-300	0.73 (0.60)	288

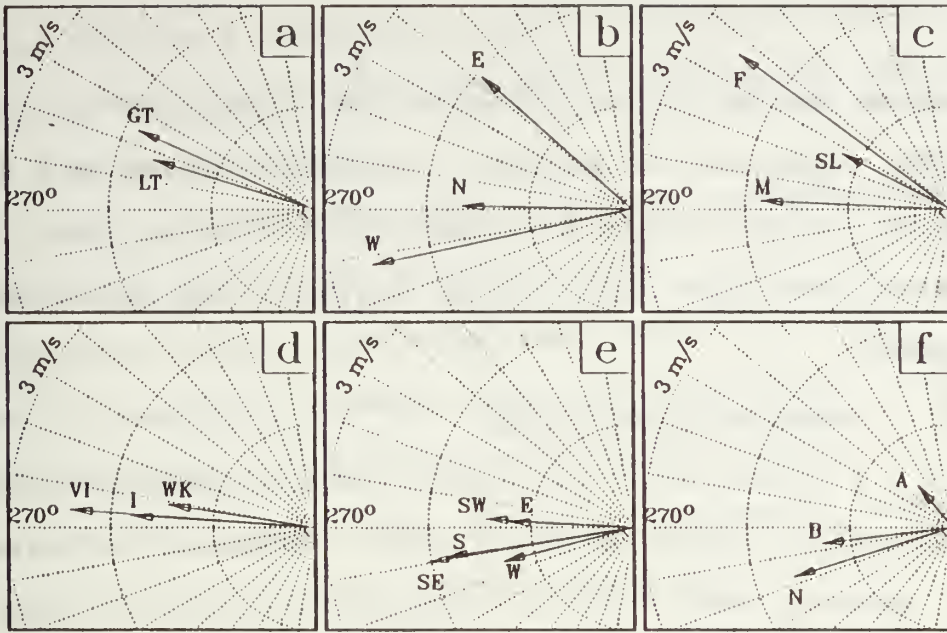


Fig. 2 Vector differences of composite tropical cyclone motion minus steering for the (a) latitude, (b) direction, (c) speed, and (d) intensity stratifications of Chan and Gray (1982), and the (e) direction and (f) recurvature stratifications of Holland (1984) after conversion to a geographical coordinate system by Carr and Elsberry (1990).

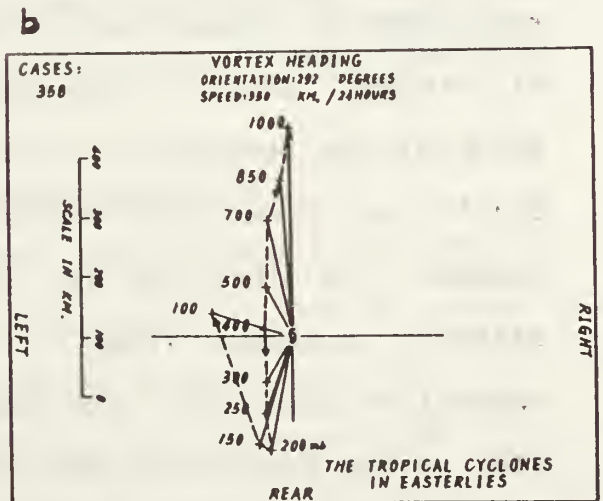
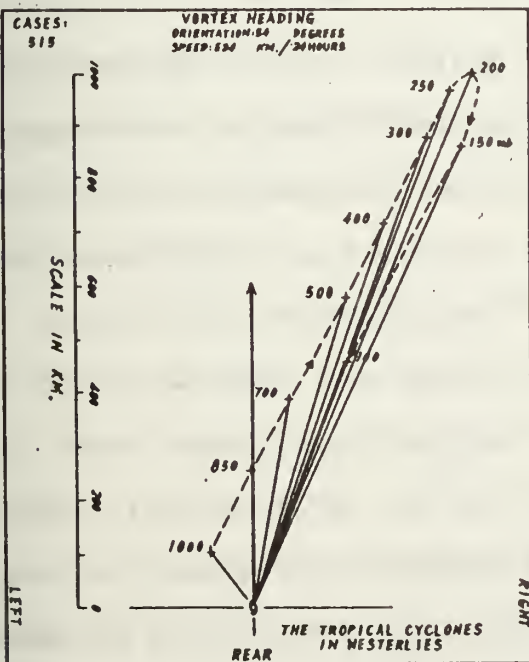


Fig. 3 Mean geostrophic wind vector at various pressures (mb) relative to the 24-h storm motion (vertical error) for (a) eastward-moving and (b) westward-moving cases in the Atlantic (Dong and Neumann 1986).

of cyclone motion minus steering are displayed in Fig. 2 for latitude, direction of motion, translation speed and intensity. Generally, these vectors have magnitudes ranging from 1-2.5 m s<sup>-1</sup> and directions that tend to be westward and poleward in each hemisphere.

b. Geostrophic steering

A geostrophic steering flow has been calculated from operationally-analyzed height fields. Neumann (1979) and Keenan (1982) demonstrated that the tropical cyclones in the Atlantic and Australian regions respectively tend to move with the speed and direction of the deep-layer environmental flow defined from such height fields. Although perhaps 80% of the 12-24 h variability in motion may be explained with steering only, the deviations can be significant.

Dong and Neumann (1986) have reanalyzed the relationship between motion and the environmental geostrophic flow at various levels. The geostrophic components are calculated from various gridpoint values of geopotential height at distances 5-10° lat. from the center. Significant differences occur between the steering for eastward-moving and westward-moving Atlantic cyclones (Fig. 3). Whereas the basic flow in the westerlies increases with height to 200 mb (Fig. 3a), the basic flow in the easterlies decreases between 1000 mb and 400 mb (Fig. 3b). Again, the departures of the storm motion from the steering defined at various pressures are quite different. Generally, the storm motion is to the left of the steering in the westerlies, but to the right in the easterlies. The mean vector differences



can not be used as a prediction scheme because the scatter about the mean is much larger than the mean differences (see Figs. 7 and 8 in Dong and Neumann).

Dong and Neumann (1986) calculate correlations between geostrophic steering at single levels and for different combinations of levels into deep-layer means (Table 2). For both westward and eastward movement, the optimum single level is 400 mb for hurricanes and 700 mb for tropical storms. Notice that the correlation coefficients between geostrophic steering and storm meridional and zonal motion range from 0.5 to 0.78. The optimum deep-layer mean is up to 100 (150) mb for westward- (eastward-) moving hurricanes. Although correlation coefficients are slightly higher with the optimum deep-layer mean rather than the optimum single layer, the 24-h track forecast errors are not significantly smaller. Dong (1988) also used the Atlantic set of Dong and Neumann (1986) plus western North Pacific data to demonstrate a correlation of 24-h displacements with cyclone intensity in the westerlies, but he found only weak dependence in the easterlies.

c. Cyclone intensity-dependent steering

Velden and Leslie (1991) demonstrate that the 850-500 mb layer provides smallest track forecast errors for Australian region storms with central pressures higher than 975 mb. For central pressures between 955-975 mb, the layer average should be from 850 -400 mb, and from 850-300 mb for the most intense storms. Gross (1991) tested the sensitivity of the Beta Advection Model (BAM) steering layer specification to cyclone

intensity. Normally, the deep-layer mean wind field for the BAM is the vertical average between 850 and 200 mb. A layer average between 850 and 700 mb provided more accurate forecasts for storms below hurricane intensity in the eastern North Pacific, and a layer average between 850 and 400 mb was better for hurricane intensity storms. In the Atlantic, the 850-400 mb layer average provided more accurate forecasts below hurricane intensity and the 850-200 mb layer was best for hurricane forecasts. Thus, studies in various cyclone basins indicate that the depth of the environmental steering flow should be increased with tropical cyclone intensity to reflect a deeper layer of cyclonic circulation.

d. Individual cases

The Synoptic-Flow Experiments by the Hurricane Research Division (HRD) of NOAA have provided adequate wind fields in individual cases by deploying Omega dropwindsondes from a flight level of about 400 mb. Lord and Franklin (1987) describe the three-dimensional, nested analysis of the wind fields. Analyses on three successive days (Franklin 1990) describe the evolution of the environmental wind field around the developing hurricane Josephine. Azimuthal-average wind vectors for the 5-7° lat. radial band indicate a large vertical wind shear (Fig. 4). Although the storm generally moves with the direction of the flow in the vicinity of 700 mb, the translation speed is approximately equal to the 500 mb (or surface to 100 mb layer mean) flow. Radial-band averages also change rapidly with increasing distance



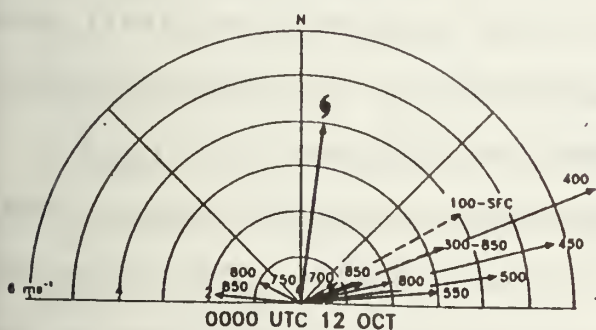
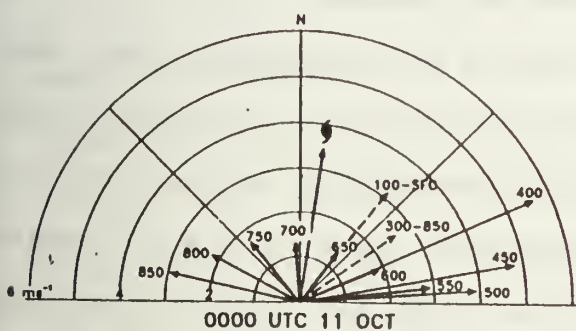
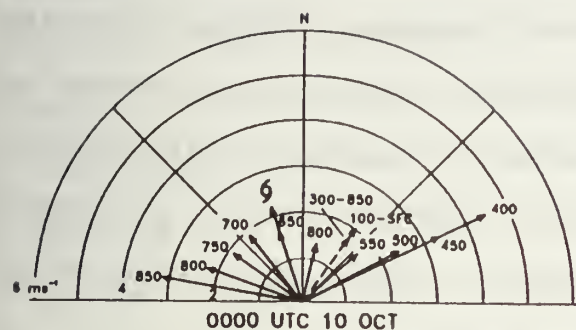


Fig. 4 Azimuthal average wind vector, for the  $5-7^\circ$  radial band, as a function of pressure. The 12-h mean motion vector of Josephine is indicated by the hurricane symbol. The figures are oriented geographically with north at the top (Franklin 1990).

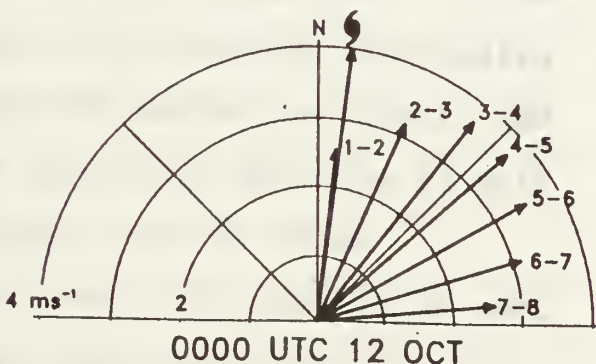
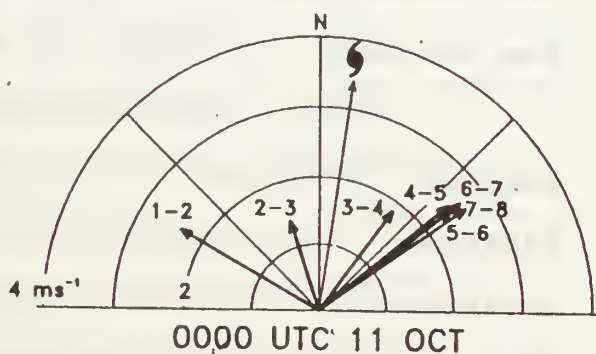
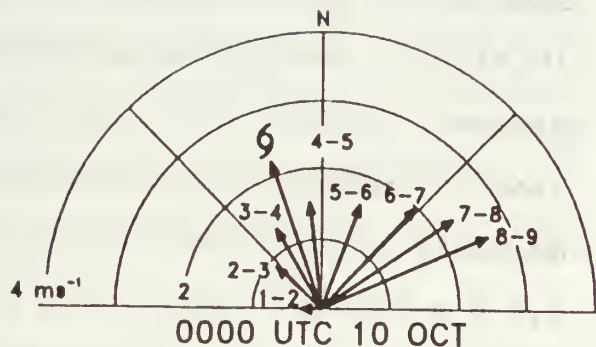


Fig. 5 Azimuthal average wind vector, for the 300-850 mb layer mean flow, as a function of radial distance from the storm center. The 12-h mean motion vector of Josephine is indicated by the hurricane symbol. The figures are oriented geographically with north at the top (Franklin 1990).

from the center (Fig. 5). While the vectors are generally similar to the rawinsonde composites of northward-moving storms in Fig. 1, the clockwise rotation with increasing radius is even greater. As the 5-7° lat. radial-band average rotates clockwise from 10 October to 12 October, the storm motion also rotates to maintain a consistent vector difference (speeds and directions: 1.8 m s<sup>-1</sup> toward 289°, 2.4 m s<sup>-1</sup> toward 319°, and 3.7 m s<sup>-1</sup> toward 317° respectively). Such consistency in time adds credence to the individual data sets and analysis techniques.

Kaplan and Franklin (1991) have applied the same analysis technique to a dropwindsonde set in tropical storm Florence. The smallest difference between the motion and the environmental flow was for the 850-500 mb layer (2.7 m s<sup>-1</sup> toward 012°). The storm motion was to the left and faster than the radial-band average at 5-7° lat. Feuer and Franklin (1991) show the difference between the storm motion and the midtropospheric flow in hurricane Gloria was toward the northwest at 2-3 m s<sup>-1</sup>.

Marks et al. (1991) have used airborne Doppler radar data to document the inner core 3-d wind field. The horizontal average of the inner core wind velocity varies with elevation due to vertical wind shear. However, the storm motion appears to agree well with the vertical mean of these areal-average wind speeds. Roux and Marks (1991) proposed a new processing technique to derive the wind field from Doppler velocity measurements along a single flight leg. Their estimates of the areal-average winds in hurricane Hugo have a nearly constant southwesterly shear between 0.5 and 8 km. The density-weighted

mean wind is  $4.9 \text{ m s}^{-1}$  from  $130^{\circ}$ ; which is very close to the average storm translation of  $3.4 \text{ m s}^{-1}$  from  $120^{\circ}$ . These new measurements confirm that the tropical cyclone is translating with the depth-averaged wind velocity in the inner core region. Such a relationship is suggested by Fig. 1. However, the relationship between the outer steering flow and this inner core steering is still unclear.

e. Mechanism for cyclone motion

Chan (1984) calculated the terms in the vorticity equation from sets of aircraft observations and from rawinsonde composite data to provide justification for the assumption of linking the maximum vorticity tendency to cyclone motion. Aircraft data in the 700-800 mb layer were composited relative to the radius of maximum winds in two groups (10-15 n mi and 20-25 n mi). In both cases, the area of maximum positive vorticity advection was in front of the cyclone near the mean radius of maximum winds. Although the divergence term modified the pattern slightly, the motion direction may be closely approximated by the advection of absolute vorticity. Rawinsonde composites provide wind data at many levels in the vertical, but have deficient coverage near the center where the maximum cyclonic vorticity advection occurred in the aircraft data. The local change in vorticity was estimated as a residual in the vorticity budget. In general, the faster the cyclone was moving, the larger the magnitude of the residual. Fast-moving cyclones tended to have similar sign tendencies over a deep tropospheric layer. In the midtroposphere, the dominant term was the horizontal advection of



absolute vorticity. Contributions from the divergence term tend to be largest in the lower and upper troposphere. Finally, subsets of the data for left-turning, straight-moving and right-turning storms tend to have consistent rotations of the horizontal advection of vorticity dipole.

Lord and Franklin (1987) used the analyzed wind fields from hurricane Debby to calculate the vorticity tendency in the surface to 200 mb layer. The horizontal advection of vorticity was the dominant term, and the divergence term was only about 25% of the horizontal advection term. The line connecting the negative-positive dipole of the vorticity advection was within  $10^\circ$  of the 12-h motion vector. Lord (1989) has examined the vorticity advection from nested analyses for other hurricanes as well. A very well-defined vorticity advection dipole that is aligned along the  $\pm 12$  h motion vector is revealed in analyses of dropwindsondes and airborne Doppler radar data in hurricane Gloria during 1985 (Feuer and Franklin 1991).

Some observational studies of tropical cyclone recurvature shed light on the environmental flow controls. Harr and Elsberry (1991) have demonstrated that the anomalous 700 mb circulation fields that exist when the tropical storm (35 kt) is named distinguishes between recurving and straight-moving track types. Although the predictions are not always correct, the results suggest that slowly varying, large-scale circulation changes affect both the genesis and the track type. Ford et al. (1991) have represented the surrounding environmental wind fields in terms of empirical orthogonal functions. Although a

separation between the recurving and straight-moving tracks is successful, the time-to-recurvature is not well forecast. Hodanish (1991) has described differences in the zonal winds in the environment of sharply recurving, slowly recurving and non-recurving tropical cyclones. Based on these differences to the northwest of the center, a prototype technique has been developed to forecast the time to recurvature.

f. Implications from observational studies

As indicated above, the focus of the recent tropical cyclone motion research studies has been on what causes the departure from the steering flow, which will be termed the propagation vector. Since the entire tropical cyclone moves coherently while being exposed to the propagation vector, this contribution to the total motion must have approximately the same scale as the cyclone (~ 1000 km diameter). On these horizontal scales, the flow through the tropical cyclone should be irrotational and thus must be part of a closed dipole circulation that has a cyclonic (anticyclonic) gyre to the left (right) of the propagation vector. This cyclonic-anticyclonic gyre pair must be rotated relative to the steering flow vector to produce the observed angular deflections of the storm motion vector. Consequently, the existence of a wavenumber one gyre circulation in the general form of Fig. 6 can be regarded as a natural consequence of the observed departure of tropical cyclone motion from the steering flow.



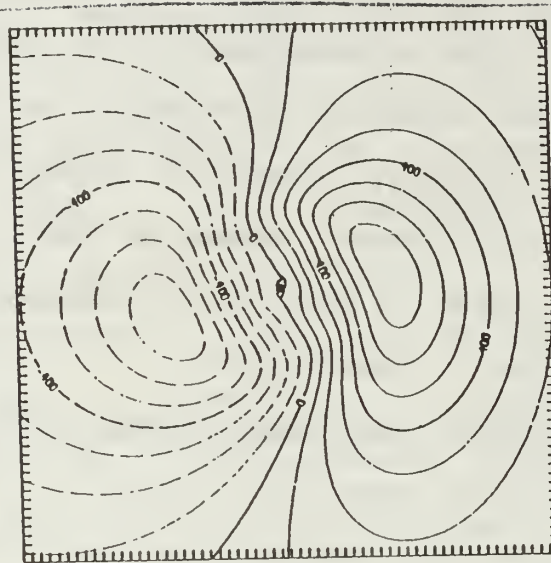


Fig. 6 Asymmetric streamfunction ( $\text{m}^2\text{s}^{-1}$ ) at 24 h in model simulation by Fiorino and Elsberry 1989a. The plot domain is  $61 \times 61$  points (with  $\Delta x = 40$  km,  $2400 \times 2400$  km) centered on the vortex. The tick marks indicate the grid points. Positive (negative) values indicate anticyclonic (cyclonic) streamfunctions. Contour intervals are  $1 \times 10^3$ , and the maximum absolute values are  $\pm 7 (10^5)$ .

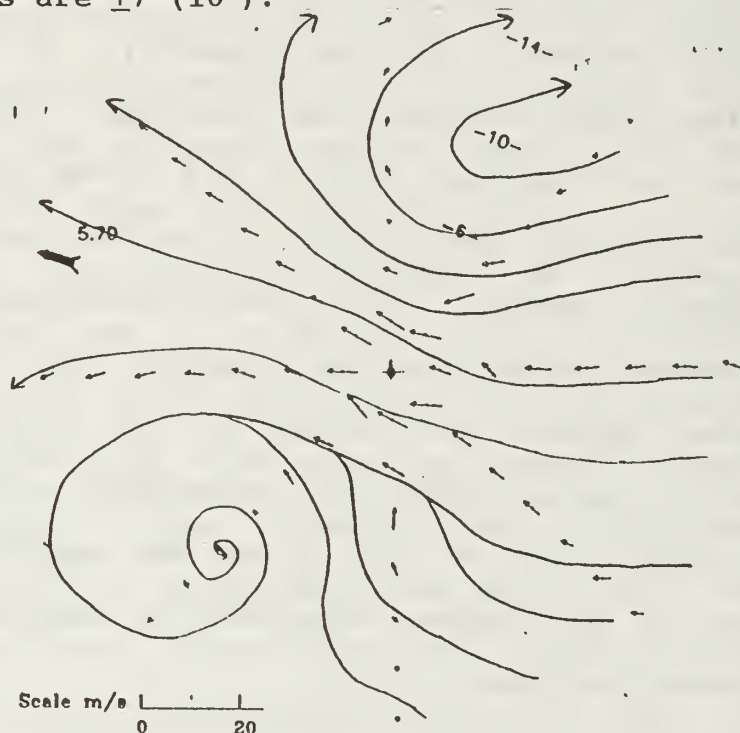


Fig. 7 Composite of rawinsonde winds averaged between 850 and 300 mb in a geographically-oriented, cylindrical coordinate system after removal of the symmetric vortex. Average direction of motion (heavy arrow) and approximate streamlines (thin arrows) for this sample of straight-moving cyclones are shown (provided by W. Gray).

A key aspect of the above reasoning is that the central region between the gyres has an essentially uniform flow of about  $1-3 \text{ m s}^{-1}$  that advects the cyclone faster and to the left or right of the defined large-scale steering flow. Rawinsonde wind composites relative to the tropical cyclone center (Fig. 7) provide support for the existence of the gyres. Although anticyclonic and cyclonic gyres of the appropriate horizontal scales appear in this composite, some of the flow shown in Fig. 7 is due to the basic current. The relationships of these observed gyres to storm structure characteristics, and environmental flow characteristics such as vorticity gradients and vertical wind shear, have been established in conjunction with analytical and numerical studies discussed in the following sections.

In most of the above observational studies, the total flow has been decomposed into the symmetric vortex that represents the existing storm structure and a large-scale flow that represents the steering. Each of these three components in the decomposition is time dependent. Although it has been assumed in most analytical models that the vortex is in steady state, the storm structure changes as the intensity and outer wind profile evolve during the life cycle. The environmental flow changes direction and magnitude as the cyclone forms in the tropics, moves around the subtropical high and recurves into the midlatitude westerlies. The asymmetric gyre circulations (Fig. 6) also will change in orientation and magnitude in response to changes in storm structure and environmental flow conditions.

The above observational studies indicate some of the basic concepts being explored in tropical cyclone motion studies. Some of the questions being addressed include: (i) How do the wavenumber one gyres such as in Fig. 6 form and do higher wavenumber gyres also form and contribute significantly to tropical cyclone motion relative to the steering? (ii) How is the region of nearly uniform flow around the center established so that the tropical cyclone moves as a coherent entity? (iii) What are the differences in shape and amplitude of the gyres with different storm structures and environmental forcing conditions? (iv) What are the adjustment times of the gyres? That is, to what extent are the gyres adjusted to the instantaneous environmental forcing conditions versus being dependent on the time history of previous conditions? (v) What is the vertical variation of the gyres and how do such vertical variations contribute to the tropical cyclone motion? (vi) How do quasi-stationary or rotating asymmetries in convection relative to the center contribute to tropical cyclone motion? (vii) How does the tropical cyclone remain quasi-vertical under conditions of environmental vertical wind shear and does vertical tilting of the low-level cyclonic and upper-level anticyclonic vortices contribute to systematic departures from the steering flow?

These questions can not be answered with the data sets available prior to the TCM-90 field experiment, and perhaps will only be detected in the TCM-90 data set if the expected distribution of the signal is known. The analytical and numerical studies described in the following sections provide

further understanding and the characteristics to be sought in the TCM-90 data set.



### 3. Beta-induced propagation

#### a. Self-advection process

Some of the basic physical processes that contribute to tropical cyclone propagation relative to the steering can be illustrated with a barotropic model in which an initially symmetric vortex is influenced only by the planetary rotation (beta effect) within a quiescent environment. Chan and Williams (1987) separately treated the linear and the nonlinear effects that contribute to the northwestward propagation at  $2-3 \text{ m s}^{-1}$ . Previous studies (e.g., Rossby 1948; Adem 1956; Kasahara and Platzman 1963; Holland 1983, 1984) had emphasized principally linear arguments to explain the propagation process. Chan and Williams (1987) demonstrated that a nonlinear self-advection (i.e., the initially symmetric vortex induces an asymmetric circulation that advects the vortex) process that explains both the westward and poleward propagation components (Fig. 8).

The propagation process can be visualized via the decomposition of the total wind field into a symmetric (S) vortex, an environmental (E) wind field that may be horizontally nonuniform, and an asymmetric (A) circulation. This asymmetric circulation develops a relative vorticity ( $\zeta_A$ ) as

$$\frac{\partial \zeta_A}{\partial t} = -\mathbf{V}_A \cdot \nabla \zeta_S - \mathbf{V}_S \cdot \nabla \zeta_A - \mathbf{V}_S \cdot \nabla (f + \zeta_E) - \mathbf{V}_E \cdot \nabla (\zeta_S + \zeta_A), \quad (1)$$

in which the environmental terms  $(\partial \zeta_E / \partial t)$  and  $\mathbf{V}_E \cdot \nabla (f + \zeta_E)$  have been omitted because they relate to the time dependence of the steering flow. The vorticity tendency in (1) is in a coordinate system centered on the symmetric vortex center. Normally, the



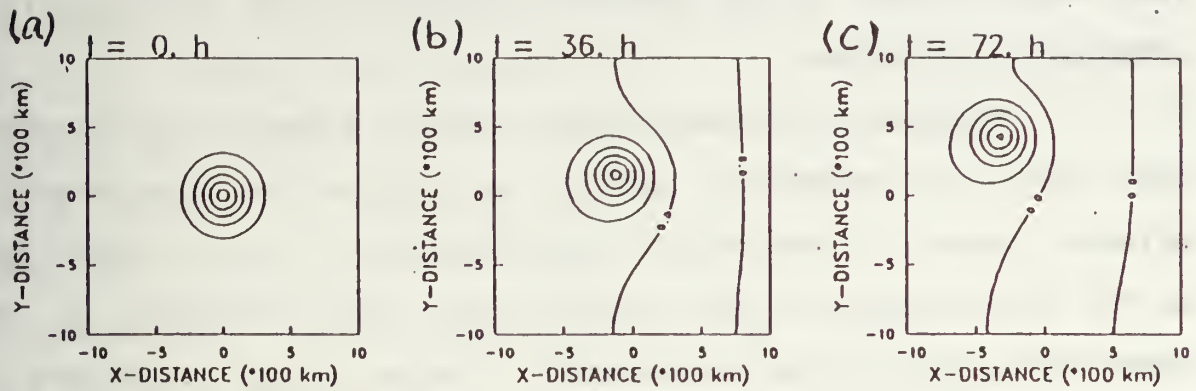


Fig. 8 Barotropic tropical cyclone structure (streamfunction) and position predicted by a nonlinear numerical model at (a) 0, (b) 36 and (c) 72 hours (Chan and Williams 1987).

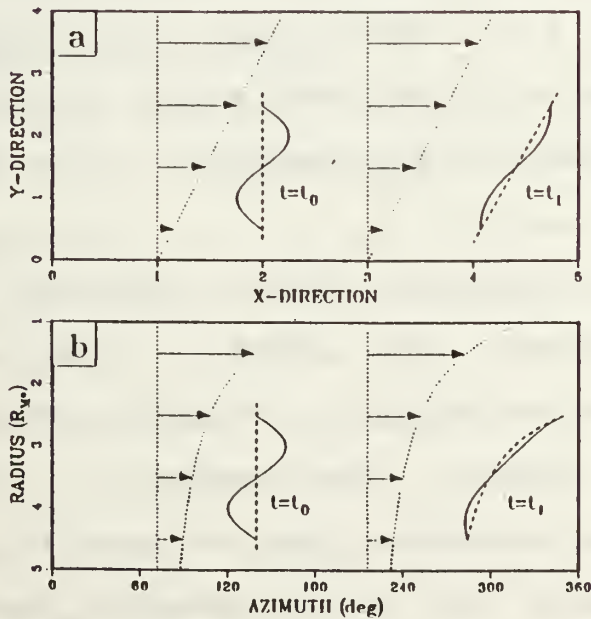


Fig. 9 Schematic portrayal of perturbation damping with time due to (a) a meridionally sheared Couette flow, and (b) a radially sheared axisymmetric vortical flow (Carr and Williams 1989).

last term in (1) is the dominant effect of the steering flow advecting the vortex.

Because Chan and Williams used a quiescent environment ( $\nabla_E = 0$ ), the propagation effect is relative to this steering effect. Since no environmental vorticity ( $\zeta_E$ ) is included and no  $\nabla_A$  or  $\zeta_A$  exists at the initial time, the advection of the earth vorticity ( $f$ ) by the symmetric vortex in the third term on the right side of (1) is the initiating effect. Chan and Williams demonstrated that this term leads to an anticyclonic (cyclonic) vorticity tendency to the east (west) of the center. That is, the poleward (equatorward) meridional wind on the east (west) side advects lower (higher) values of earth vorticity. This east-west dipole of vorticity tendency generates only a small (less than  $0.5 \text{ m s}^{-1}$ ) Rossby wave-like propagation toward the west. More importantly, this beta effect distorts the vortex and generates the asymmetric flow essential to the self-advection process.

Fiorino and Elsberry (1989a) illustrated the separate roles of the self-advection terms (first two terms on right side) by calculating the  $\nabla_S$  and  $\nabla_A$  from a numerical model similar to Chan and Williams (1987). The asymmetric circulation is predominantly due to wavenumber one and consists of the two counterrotating gyres in Fig. 6. An essential feature of this circulation is the near-uniform flow between the gyres that advects the entire vortex. Fiorino and Elsberry demonstrate that the average velocity of the uniform flow is almost equal to the translation speed of the center (Fig. 8). Since the environment

is quiescent, the propagation vector is due entirely to  $-\nabla_A \cdot \nabla \zeta_S$ . The second self-advection term in (1) is also important. Fiorino and Elsberry show how this term cyclonically rotates the inner portion of the gyres in Fig. 6, while the outer gyres continue to be oriented more east-west. Moreover, the streamfunction tendency associated with  $-\nabla_S \cdot \nabla \zeta_A$  nearly cancels the tendency associated with the beta term when a quasi-steady state is achieved after about 12 h. Whereas the primary influence of the beta term is to generate the asymmetric circulation, the  $-\nabla_S \cdot \nabla \zeta_A$  term limits the growth of the wavenumber one gyres. As these two effects come into balance, the uniform-flow region between the gyre centers achieves quasi-equilibrium so that the propagation vector ( $-\nabla_A \cdot \nabla \zeta_S$ ) is quasi-steady.

b. Uniform-flow region

Another essential feature of the near-uniform flow between the gyres is the barotropic stabilization process that has been described by Carr and Williams (1989). Because the persistent asymmetric forcing associated with the beta term would eventually deform the vortex (see Chan and Williams 1987), a stabilization mechanism that maintains the vortex over the long periods that a tropical cyclone exists is thus essential. Carr and Williams (1989) illustrate the physical process by which nonlinear advection stabilizes the vortex via the radially sheared axisymmetric flow (Fig. 9). They impose perturbations with appropriate azimuthal wavenumbers ( $k=1, 2, \dots$ ) and different radial profiles to represent the beta-induced asymmetry and other asymmetries associated with shear and latitudinal



gradients in environmental relative vorticity, convection near the center, etc. As indicated schematically in Fig. 9, the shear due to the increasing winds toward the center of the tropical cyclone vortex damps the perturbation with time by stretching it through differential advection. The key question is how rapidly each type of initial perturbation is damped.

Carr and Williams demonstrate that barotropic stabilization occurs because the perturbation tilts with the horizontal shear so that perturbation kinetic energy is transferred to the basic state represented by the symmetric vortex. The energy conversion rate is proportional to the (inward) eddy momentum flux and the shear of the angular wind speed ( $v/r$ ). Thus, the radial distribution of the perturbation is quite important because the angular wind speed is very large near the center and decreases rapidly with radius. Perturbations induced by eyewall convection will be damped with a time scale of a few hours. Carr and Williams also show that perturbations with a higher azimuthal wavenumber damp faster than those with a low wavenumber having the same radial structure. For a non-forced beta-like asymmetry that has maximum amplitude hundreds of kilometers from the center, the damping is slower because the angular wind speed is small at these radii (Fig. 10). Without the forcing that maintains these beta-like gyres in an east-west orientation, the gyres are rotated cyclonically by 8 h. Notice that the inner region has become axisymmetric by 36 h, and only the outer region of the gyres still remain at this time. This asymmetry-damping mechanism acts as a negative feedback process



in which kinetic energy transfer from the asymmetric to the symmetric component of the vortex opposes the energy transfer from the symmetric to the asymmetric component induced by an external forcing such as the beta effect.

Shapiro and Ooyama (1990) provide a nice demonstration of how the shear-induced adjustment process leads to a homogenization of absolute asymmetric ( $k=1$ ) vorticity within the region between the gyre centers (Fig. 11). The region within 350 km of the center has a near-uniform southward vorticity gradient that is nearly equal in magnitude (but opposite in sign) to that of the Coriolis parameter. Consequently, the region within 350 km has near zero absolute vorticity gradient for the  $k=1$  asymmetry. Outside the region, the relative vorticity is negative (positive) to the east (west) in conjunction with the anticyclonic (cyclonic) gyres. The absolute vorticity values (Fig. 11b) illustrate the advection of smaller (larger) values from the equatorward (poleward) side on this beta-plane, which established the gyres. Only within the inner region of large radial shear in angular wind is the barotropic stabilization and the homogenization process effective.

In the non-divergent barotropic model, the absolute vorticity must be conserved following the parcels. Under the influence of the large radial shear in angular wind speed near the cyclone center, the vorticity perturbation will be wrapped around the center more rapidly near the center (Fig. 10). As the radial length scale is decreased, the velocity amplitude also must decrease to conserve the vorticity along the path. Thus,

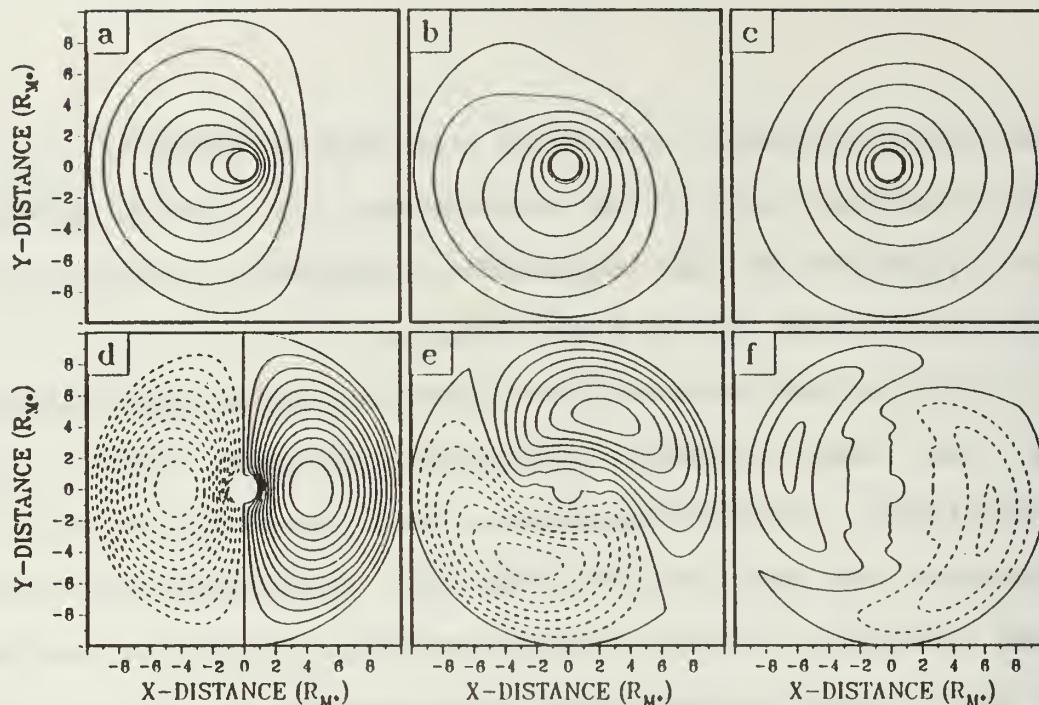


Fig. 10 (a)-(c) Perturbation plus symmetric streamfunction for a  $\beta$ -induced asymmetry at  $t=0$ , 8 and 36 hours, respectively. Contour interval is  $7.4 \times 10^5 \text{ m}^2 \text{ s}^{-1}$ . (d)-(f) Same as (a)-(c) except showing just the perturbation streamfunction (solid, positive; dashed, negative), and using a contour interval of  $1.7 \times 10^5 \text{ m}^2 \text{ s}^{-1}$  (Carr and Williams 1989).

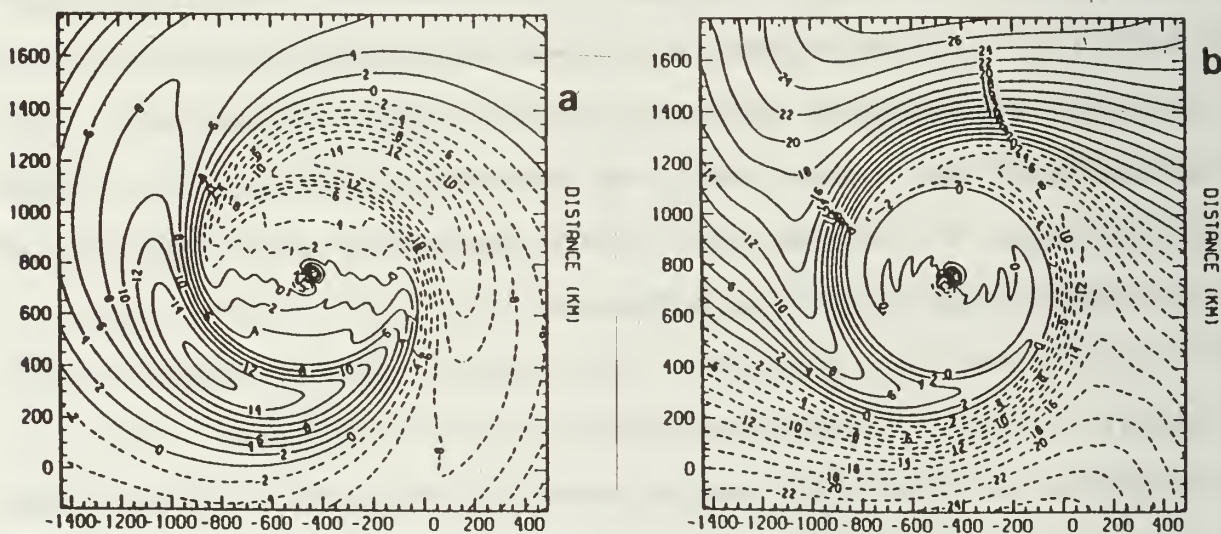


Fig. 11 Wavenumber 1 asymmetric component in Shapiro and Ooyama (1990) beta-effect experiment at 120 h. (a) vorticity  $\zeta'$  ( $k=1$ ) [contour interval  $2 \times 10^{-6} \text{ s}^{-1}$ ]; and (b) absolute vorticity,  $\beta (Y-Y_c) + \zeta' (k=1)$  [contour interval  $2 \times 10^{-6} \text{ s}^{-1}$ ].

the inner part of the asymmetric circulation (wavenumber one gyres) in Fig. 6 has a near-uniform speed that advects the entire inner region of the symmetric vortex at the same speed, so the vortex maintains integrity. As Shapiro and Ooyama (1990) conclude: neutralization of the beta effect by the asymmetries "isolates" the vortex and allows it to move relatively undistorted by environmental influences.

Shapiro and Ooyama (1990) note that the homogenization of absolute asymmetric vorticity does not occur inside the radius of maximum winds, where the angular velocity is nearly independent of radius because of the solid-body rotation. Consequently, the barotropic stabilization process of Carr and Williams (1989) does not apply, and induced asymmetries simply rotate about the center.

### c. Analytical models

Carr (1989) derives analytical expressions for the wavenumber one gyres as a function of radius. Carr separately treats an inner Self-advection Region where mutual advections by the symmetric vortex and the asymmetric gyre circulation [terms 1 and 2 on right side of Eq. (1)] are important, and an outer Dispersion Region where such advections are unimportant. These solutions must be matched at the transition radius between these two regions. At least two radial annuli are used between the radius of maximum winds and the transition radius, and again the solutions must be matched at the interface. The symmetric tropical cyclone wind field may be approximated by a analytical modified Rankine profile



$$v_s(r) = D_0 r^{-x} + D_1 (r-1) + D_2 (r-1)^2 + D_3 (r-1)^3, \quad (2)$$

where the radius is scaled by the radius of maximum winds. A key requirement is that vorticity gradient must be well represented at the transition radius and other interfaces.

The propagation vector may be specified externally, or Carr provides an internally consistent propagation that may be used as a first approximation. Although the internal closure scheme for the propagation vector assumes a quiescent environment, the general streamfunction solution includes the effects of linear shear or relative vorticity gradients in the large-scale environment. An 8 x 8 linear system of equations for the value and first derivative of the complex streamfunction in the wavenumber one gyres is solved to match all of the interface and boundary conditions. An iterative solution with a single adjustment parameter is found that satisfies a condition that the magnitude of the asymmetric vorticity is continuous at the transition radius. The streamfunction equations and details of the solution method can be found in Carr (1989), who uses the analytical model to indicate the dominant physical processes.

An innovative modeling approach by Willoughby (1988) provided insights into the track effects due to rotating mass sources/sinks, but it predicted an unrealistic translation speed ( $105 \text{ m s}^{-1}$ ) when beta forcing was imposed. This shallow-water model was formulated in cylindrical coordinates moving with the storm center. Only the azimuthal wavenumber one (associated with tropical cyclone motion as shown above) was treated in the linear version of the model. The asymmetric perturbations in this model



are linear Rossby waves that propagate on the radial gradient of potential vorticity associated with the shear of the symmetric vortex circulation. The vortex moves through its environment, which causes a slipstream flow around the uniform flow region of the vortex. In Willoughby (1988, 1990), the vortex motion is determined variationally from Hamilton's principle. More recently, Willoughby (1991) uses the asymmetry of the solution calculated in small time steps (five minutes) to detect apparent asymmetries due to a change in translation from the previous estimate. The erroneous solution for the beta forcing case in Willoughby (1988) has led him to a normal mode explanation of the problem, and the normal modes may be used to interpret the predicted vortex motion for a number of forcing effects (Willoughby 1991). The key to more realistic simulations of motion and structure has been to relax the steady-state assumption in the original model and to examine the transient response of the normal modes (Willoughby 1991).

Smith et al. (1990) describe the evolution of the vorticity fields in a nondivergent barotropic model, and show how the homogenization of the vorticity fields (as in Carr and Williams 1989) in the inner regions invalidates simple scale analyses of the vorticity equation. They introduce an analytical theory for the development of the gyre structure when a symmetric vortex is suddenly imposed on a beta-plane at time zero. Smith and Ulrich (1990) further analyze this essentially linear Lagrangian model in which relative vorticity changes are computed for particles moving in circular orbits relative to the moving

vortex. They also assume that the vortex center is advected by the asymmetric streamflow across it, as demonstrated by Fiorino and Elsberry (1989a). The theory predicts gyre structures that agree with the numerical calculations up to about 24 h. This theory is not complete in that it does not apply at large distances from the center where the tangential velocities are comparable with or less than the vortex translation speed, and the propagation direction and speed are not predicted.

In a forthcoming paper, Smith (1991) extends the theory to include the effects of environmental shear and relative vorticity gradients, and the gyre structure compares favorably with a numerical model by Ulrich and Smith (1991). These environmental effects will be discussed below in Section 5.

A fourth analytical model for the asymmetric circulation associated with a vortex moving on a beta-plane is the linear, nondivergent barotropic model of Peng and Williams (1990). The axisymmetric part of the vortex is treated as a constant basic state in a moving coordinate system following the vortex, and the system is linearized with respect to this basic state. In contrast to the Carr (1989) and Willoughby (1988, 1990, 1991) models, the propagation speed and direction must be specified from external information, which was also the case with the Smith and Ulrich (1990) model. The model steady-state solution for the beta gyres is oriented in the same direction as the specified movement and resembles the numerical model solution if proper outer boundary conditions are also specified.

An analytical model on a beta-plane of the self-induced translation of an intense vortex relative to a uniform background flow has been developed by G. G. Sutyrin (1987, 1988, 1989). A reduced-gravity, quasi-geostrophic approximation is used with a polar coordinate frame translating with the vortex center. As in the Willoughby model, the linear wavenumber one response to the forcing is the sum of stationary parts and an oscillatory part that rotates about the vortex. Expressions are derived for the Rossby wave drift and a dipolar component, which leads to an asymmetric circulation that is responsible for the relative vortex motion. The analytical solution for beta forcing is similar to numerical model solutions.

d. Effect of divergence

Both nondivergent barotropic and single layer (shallow water) primitive-equation models that allow divergence have been used to study the beta effect on vortex propagation. Shapiro and Ooyama (1990) demonstrated that nearly identical tracks are produced (Fig. 12), which contradicts an early result by Anthes and Hoke (1975) that divergence caused a significant slowing of the translation. After a 72 h displacement of about 500 km, the track difference is only 21 km. Shapiro and Ooyama use a scale analysis of the vorticity equation to support the small effect of divergence when the horizontal length scale is small compared to a local Rossby radius of deformation. The conclusion must be that the track differences noted by Anthes and Hoke were due to different initial wind structures in the nondivergent and divergent models.

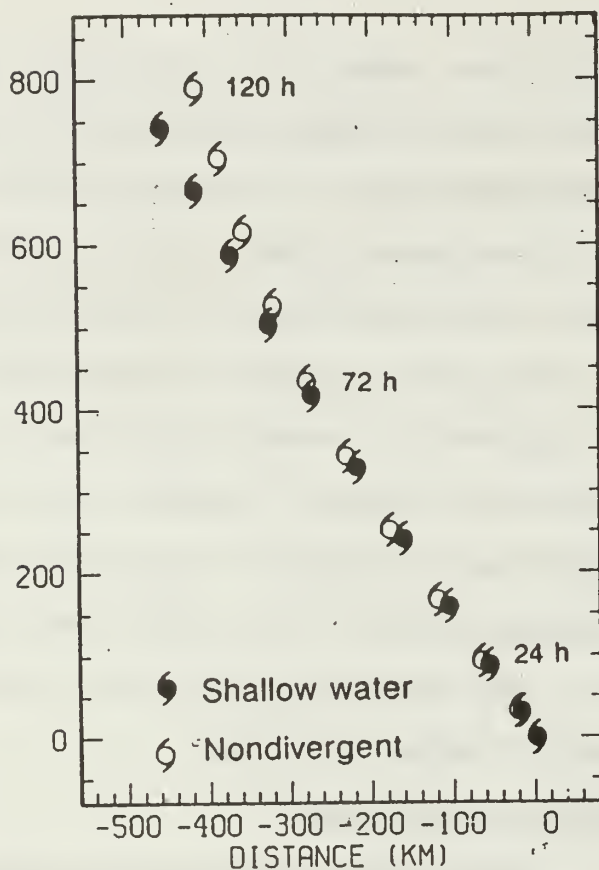


Fig. 12 Positions of vortex center every 12 h for beta-effect experiment with cyclonic vortex in shallow water and nondivergent models (Shapiro and Ooyama 1990).

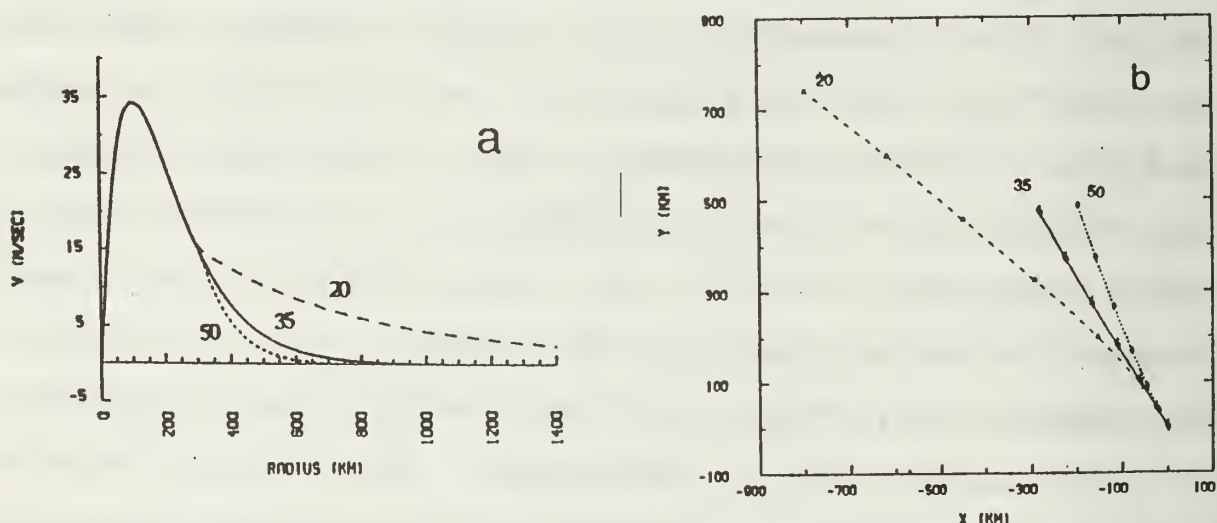


Fig. 13 (a) Tangential wind profiles with identical inner profiles and maximum intensity of  $50 \text{ m s}^{-1}$  (short-dashed),  $35 \text{ m s}^{-1}$  (solid) and  $20 \text{ m s}^{-1}$  (long-dashed) and (b) corresponding tracks to 72 h with the same line pattern as used in (a) and symbols along the tracks each 12 h (Fiorino and Elsberry 1989).



#### 4. Vortex structure effects

Most of the studies that have addressed the influence of tropical cyclone wind structure have used barotropic models forced by the beta effect as in Section 3. Because the structure effects are an important result that probably has application to real cyclones, a separate section is used to highlight these conclusions.

##### a. Outer wind effect

DeMaria (1985; see also Holland 1983) has demonstrated that the propagation effect is dependent on the outer vortex structure. Fiorino and Elsberry (1989a) confirm (Fig. 13) that the propagation depends strongly on the outer wind profile (related to strength), but is almost independent of the inner wind changes (intensity). A vortex with a larger outer wind strength has a faster and more westward propagation. Various tangential wind profiles as in Fig. 13 will be mapped differently into the small-, medium- and large-scale components of the wind analysis. Fiorino and Elsberry (1989b) concluded that the propagation speed is determined primarily by the large-scale component (mainly outer wind strength), whereas the propagation direction is determined primarily by the medium and small scales, which influence the orientation of the asymmetric gyres. The forecasting implication is that a large typhoon in a weak environmental flow may be expected to have a much larger deviation from steering, whereas a small cyclone in a strong environmental flow may be explained almost entirely by the steering concept.

strength dependence illustrated by Fiorino and Elsberry (1989b)

One interpretation of the vortex structure effect is given by the barotropic vortex stability mechanism of Carr and Williams (1989). In terms of (1), an increase in outer wind strength amplifies the asymmetry-producing influence of earth vorticity advection (beta effect), which should increase the distortion of the vortex. The beta effect is largest at outer radii where the self-advection terms are small. By contrast, the self-advection terms are largest near the center and become even more effective for larger intensities, which increases the shear of the angular wind speed. Thus, the barotropic stabilization effect neutralizes any effect of such intensity increases. However, the counterbalance to outer winds increasing the asymmetric forcing of the beta effect must be an increased down-shear tilt, which means the inner flow region must be twisted more cyclonically to maintain a quasi-steady deformity. Since this inner region of the asymmetric circulation governs the direction of the vortex propagation, the vortex with larger outer wind strength has a more westward propagation (Fig. 13).

b. Relative angular momentum relationships

Willoughby (1988) proposed that the poleward component of the propagation will be proportional to the area-integrated relative angular momentum ( $rv$ ) of the vortex. However, Shapiro and Ooyama (1990) showed that propagation on a beta-plane does not depend on initial relative angular momentum (RAM) in a straight-forward way. This is probably because RAM is an integral measure that is not uniquely related to the outer wind strength dependence illustrated by Fiorino and Elsberry (1989a).

The profiles in Fig. 13 all have positive RAM because the winds are all cyclonic. However, only light anticyclonic winds at outer radii are sufficient to reduce the RAM to zero because of the  $r^2$  dependence in the areal integration. One interesting feature of a vortex with  $RAM = 0$  is that the vortex is isolated in the sense that no significant Rossby wave radiation occurs (Flierl 1983). Thus, the vortex will not interact with the environment and potential problems with distortion effects near the boundaries due to Rossby wave radiation are avoided. Shapiro and Ooyama (1990) used a large domain with seven nested grids to demonstrate the absence (presence) of a Rossby wave wake region behind a zero (positive) RAM vortex. Willoughby (1990) shows that a zero RAM vortex has waves emanating from the cyclonic and anticyclonic circulations interfere destructively so that no momentum flux reaches the periphery to form the wake.

Fiorino (1987) noted a consistent tendency for development of anticyclonic winds at large radii in all integrations begun with positive RAM vortices. Extremely long integrations (10-15 days) always resulted in an equilibrium wind profile that tended toward zero RAM. Carr and Williams (1989) demonstrated that the radius of the maximum inward momentum flux in the barotropic stabilization process moved outward for 48 h. Outside (inside) this radius, the symmetric wind became more anticyclonic (cyclonic) with time due to momentum flux divergence (convergence). Therefore, the RAM decreased in time. Such a decrease is required in a nondivergent, barotropic model in which



parcels conserve absolute vorticity and the cyclone is moving poleward, because some compensating negative vorticity is then necessary.

Shapiro and Ooyama (1990) show that the slow decrease in RAM within a radius of 1000 km is due to a near-balance between a negative (anticyclonic) Coriolis torque and a positive (cyclonic) angular momentum flux. The Coriolis torque is negative because the southerly component of the flow between the gyres exports higher Coriolis values on the north side compared to the import on the south side. The angular momentum flux across the 1000 km circle is due to inward (outward) flow of cyclonic (anticyclonic) momentum to the northwest (southeast). At larger radii, the Coriolis torque term is dominant and the RAM within these radii tends to have large oscillations due to the development of successive anticyclonic gyres at larger and larger distances in the Rossby wave wake behind the vortex. These nonlinear processes, and the dependence of the RAM value on the areal domain, prevent any simple relationship between the initial RAM and its changes in time.

Willoughby (1990, 1991) illustrates the large and small poleward speeds (Fig. 14a) of positive and zero RAM vortices respectively due to the beta effect in his linear model. The asymmetric streamfunction associated with the positive RAM vortex after 10 days (Fig. 14b) is similar to Fig. 1 except the uniform flow between the gyres corresponds to a translation speed of  $9 \text{ m s}^{-1}$ . In this linear model with only wavenumber one in the azimuthal direction, the motion accelerates rapidly to  $2 \text{ m s}^{-1}$



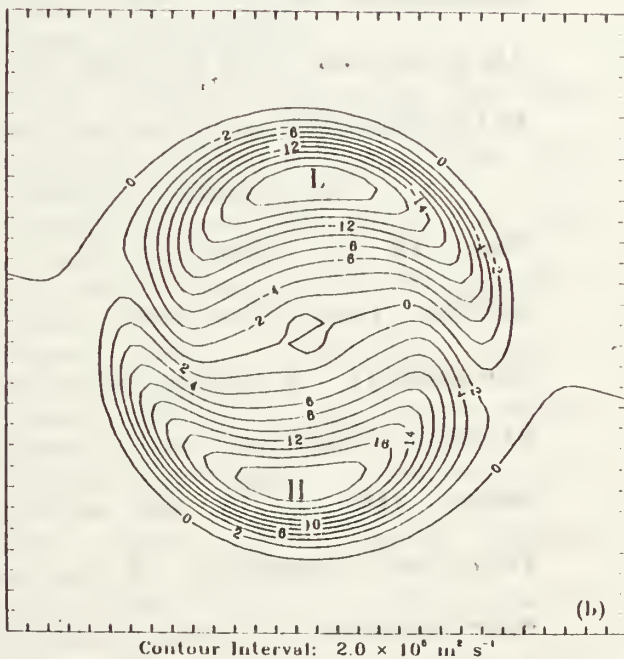
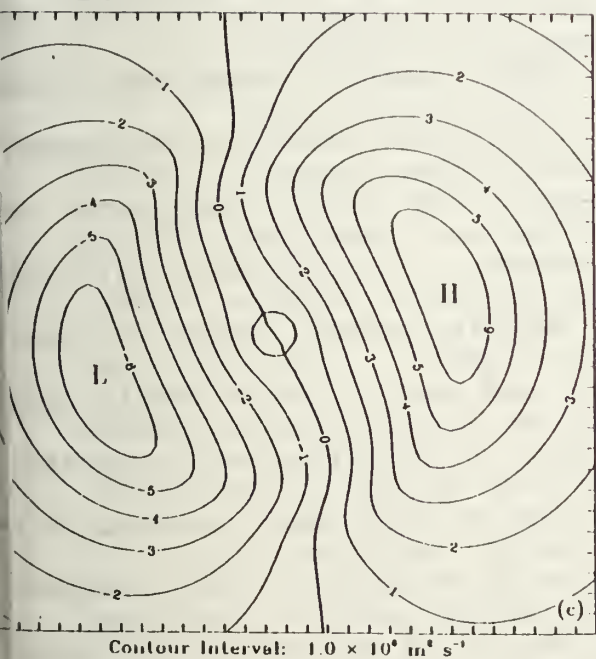
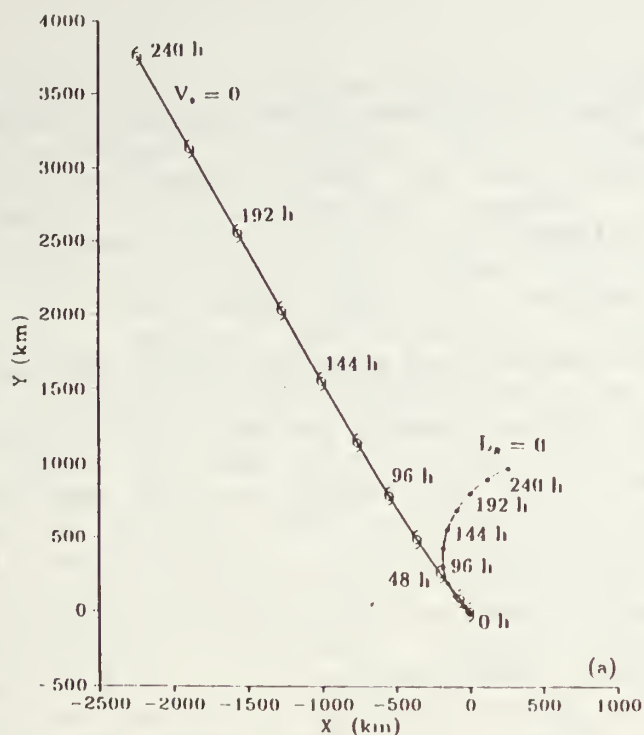


Fig. 14 (a) Vortex tracks on a beta plane for a completely cyclonic vortex ( $v_0 = 0$ ) and for a zero relative angular momentum vortex ( $L_R = 0$ ) in Willoughby (1991) model. Wavenumber one streamfunctions for (b) cyclonic vortex and (c)  $L_R = 0$  vortex after 240 h.

during the first 24 h, and then assumes a constant acceleration to  $9 \text{ m s}^{-1}$  after 240 h. The orientation of the gyres and the propagation direction toward  $330^\circ$  remain steady after an adjustment period of less than 24 h. The asymmetric streamfunction associated with the zero RAM vortex (Fig. 14c) is confined to a smaller domain (within the cyclonic tangential wind region) after 240 h and has a smaller amplitude and different orientation than Fig. 14b. Again, the translation speed increased rapidly during the first 24 h to about  $1 \text{ m s}^{-1}$ , and then had a steady acceleration to  $2 \text{ m s}^{-1}$  after 10 days. As indicated in Fig. 14a, the track direction is rotating anticyclonically with time, and the gyre orientation in Fig. 8c is rotating in a similar fashion. After about 30 days, the track will complete a cycle as the gyre orientation rotation continues.

Willoughby (1991) interprets the tracks and gyres in Fig. 14 in terms of the normal modes. A completely cyclonic vortex (positive RAM) has three stable normal modes at zero frequency. A vortex with near-zero RAM has a single stable mode at zero frequency and a conjugate pair of barotropically unstable modes with a 75 day e-folding time at the most anticyclonic rotation frequency of the symmetric circulation. The constant acceleration of the positive RAM vortex is attributed to large forcing due to the beta effect at near-zero frequency, which is similar to forcing of a harmonic oscillator at the resonant frequency. That is, the linear calculation of motion on a beta plane does not reach a steady state, so that the propagation speed becomes excessive given sufficient time. In the zero RAM

vortex case, the period and growth rate are nearly equal to a barotropically unstable resonance at the most anticyclonic rotation frequency of the symmetric vortex. As the unstable normal mode grows and rotates, the gyre structure in Fig. 14c grows and rotates. Notice that this gyre has trailing spirals centered just inside the zero crossing between the cyclonic and anticyclonic parts of the mean vortex circulation, and the streamfunction is nearly zero outside the symmetric vortex region. Although the results of the linear model of Willoughby are not realistic for such 10-day integrations, the interpretation in terms of normal modes proves useful for understanding other types of forcing besides the beta effect.

c. Possibility of observational validation

In each of these barotropic models forced by the beta effect, a strong sensitivity of the propagation to the outer wind profile has been demonstrated. The analytical model of Carr (1989) requires a careful specification of the radial gradient in the vorticity. Peng and Williams (1990) illustrate that a steady-state solution of their linear model in the inner region (where the vorticity gradient is negative) leads to another pair of counterrotating gyres. These inner gyres have maximum amplitude at the radius of maximum winds and are not oriented along the specified translation direction. Only if these inner gyres are suppressed will the outer gyres in Fig. 6 be reproduced. The balance of the terms in the vorticity equation requires that the relative vorticity gradient be positive, which is true outside 325 km for the wind profile used by Peng and

Williams. A normal mode stability analysis (Peng and Williams 1991) for the symmetric wind profile demonstrates that the existence of an unstable or a neutral mode for wavenumber one is dependent on the proper resolution of the vorticity gradient. Weber (1991) also sought the unstable linear modes for various wind profiles that have been used in tropical cyclone motion studies. Whereas the profiles for large vortices had no unstable modes, the small vortex had a wavenumber two instability that might feedback into the wavenumber one mode that governs the motion.

Such a sensitivity of the models to the wind profile (and its first and second derivative in the vorticity and vorticity gradient respectively) makes observational verification of these results rather difficult. Composite studies can not be used because they average over many storms. Fortunately, a detailed knowledge of the inner core wind profile is not required. However, the outer wind profile must be specified carefully. This is outside the region of normal aircraft reconnaissance, so that the wind fields must be derived using remote sensing techniques. Since these models are barotropic, a deep-layer mean wind field is required. As indicated earlier, the layer depth over which the winds should be integrated is still uncertain and may be dependent on the cyclone intensity. However, the main point to be emphasized is that the propagation will depend on the outer wind profile.



## 5. Environmental relative vorticity gradient and shear

### a. Relative vorticity gradient

An environmental relative vorticity gradient will enhance or diminish the beta effect in the third term on the right side of (1). DeMaria (1985) showed that the symmetric vortex circulation advecting the absolute vorticity gradient did indeed increase the meridional deflections relative to the beta effect only (Fig. 15). For the sinusoidal variation in zonal wind in Fig. 15a, the latitudinal gradient of relative vorticity is positive (same sense as beta) at point A and negative at point B. On an  $f$ -plane ( $\beta = 0$ ), the poleward (equatorward) deflection at point A (B) is consistent with the third term in (1). This effect is superposed on the eastward (westward) advection by the basic flow at point A (B). When the beta effect is added, an additional poleward deflection occurs at point A due to the larger absolute vorticity gradient. At point B, the poleward deflection associated with the beta effect overwhelms the equatorward deflection due to the environmental relative vorticity gradient, rather than simply neutralizing the effect by virtue of a smaller absolute vorticity gradient. Shapiro and Ooyama (1990) also examine the effect of a sinusoidal wind profile. Whereas a larger poleward deflection occurs at a location analogous to point A in Fig. 15a, the deflection slows and becomes equatorward after 72 h, which suggests that additional effects are occurring.

DeMaria (1985) also demonstrates that an increasing (decreasing) relative vorticity gradient with latitude can lead

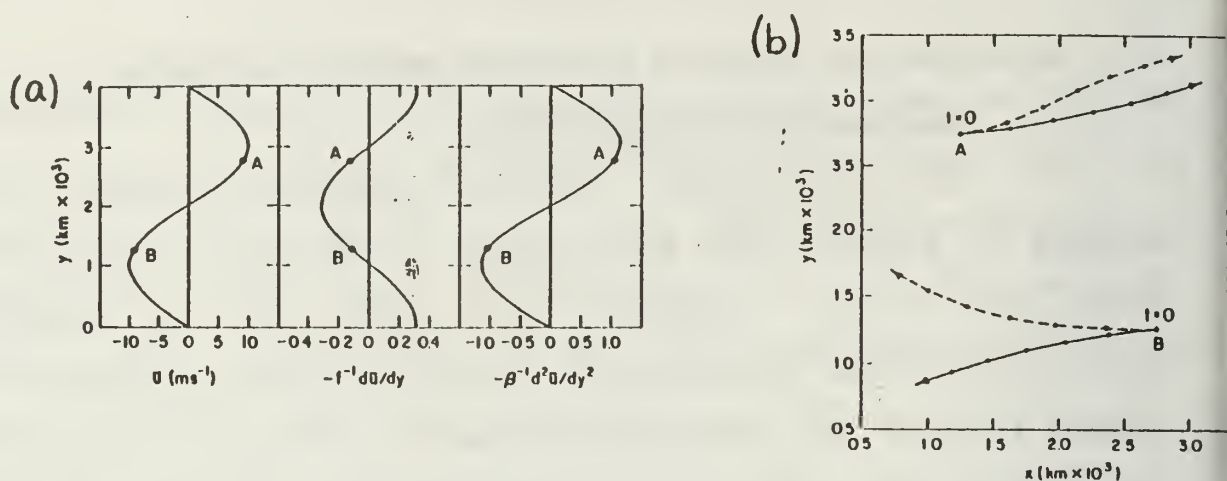


Fig. 15 (a) Sinusoidal zonal current on a beta-plane and associated absolute vorticity and vorticity gradient. (b) Tracks predicted by nondivergent spectral model for initial locations A and B in zonal current for (a)  $f$ -plane (solid) and beta-plane (dashed) approximations (DeMaria 1985).

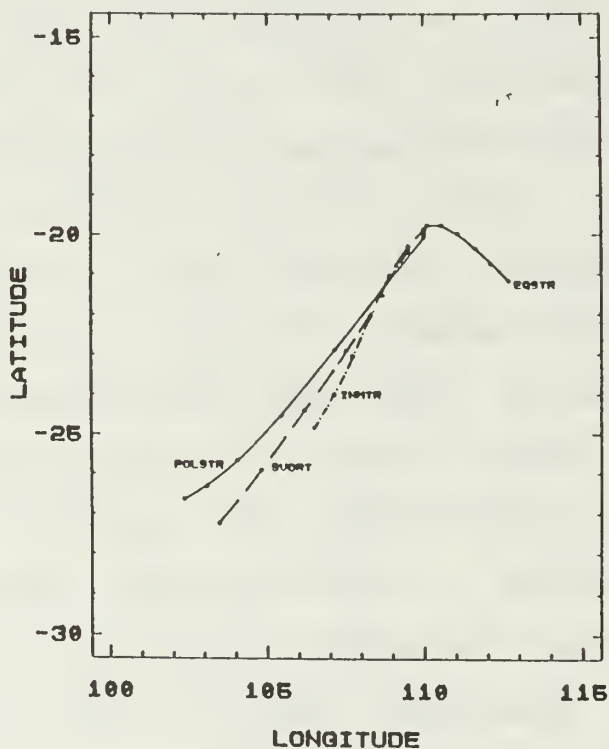


Fig. 16 72-h propagation of the vortices after removing the advection associated with the original zonal flow for initial positions poleward (POLSTR) and equatorial (EQSTR) of subtropical ridge and in monsoon trough (INMTR) compared to no mean flow (SVORT) case (Evans et al. 1991).

to diverging (converging) vortex tracks with time. Li and Zhu (1991) drew a similar conclusion from their numerical model experiments with different environmental flow backgrounds. If such high-order derivatives of the wind field ( $\nabla^2 \zeta_a$ ) could be observed, a forecaster might be able to anticipate where dynamical track forecasts would be most sensitive to initial position errors.

Evans et al. (1991) examine the motion of a large vortex in the vicinity of a strong subtropical ridge (relative vorticity gradients of same magnitude as beta). After removing the advection associated with the original zonal flow, the vortex displacements are to the west (east) of the track of a vortex in a quiescent environment if the initial position is poleward (equatorward) of the subtropical ridge (Fig. 16). Whereas the vortex propagation is highly correlated with the absolute vorticity gradient at early times, the correlation decreases with time. First, the initial cyclonic symmetric vortex is modified significantly at outer radii to decrease the RAM, which reduces the propagation vector. Second, the near-zero absolute vorticity regimes lead to erratic reversals in propagation direction as the vortex is deflected over small distances. Finally, the presence of the vortex modified the environment, which also changes the propagation. Nevertheless, Evans et al. suggest that propagation is linearly related to the absolute vorticity gradient to at least first order. Ulrich and Smith (1991) and Smith (1992) argue that the shear contribution is sufficiently large that the propagation can not be a function of absolute vorticity gradient

alone. It appears that the northern boundary of the Ulrich and Smith numerical model is already distorting the wavenumber one gyres by 24 h (see their Fig. 7c). Consequently, this distortion may invalidate their comparisons of propagation vectors with the absolute vorticity gradients. More information is required on their method of calculating these gradients in view of the significant vorticity values associated with the asymmetric circulation.

One interesting environmental relative vorticity gradient specified by Ulrich and Smith (1991) and Williams and Chan (1991) is that equal to positive or negative beta. Contrary to intuition, the displacements are not the same as the beta effect in a quiescent environment (Fig. 17). When the mean zonal advection is removed, the relative vorticity gradient equal to a positive beta results in a slower and more westward track. The vorticity gradient equal to a negative beta results in a southeastward track that is opposite to the positive beta case. Williams and Chan assert that the inclusion of a relative vorticity gradient introduces a term that adds to the beta effect in the inner portion of the vortex, and subtracts in the outer part. If the outer wind speeds are effectively reduced, the gyre amplitudes will be reduced (as in Section 4), which is consistent with the smaller displacements in Fig. 16. Williams and Chan conclude that the vortex propagation can not be just a function of the absolute vorticity gradient.



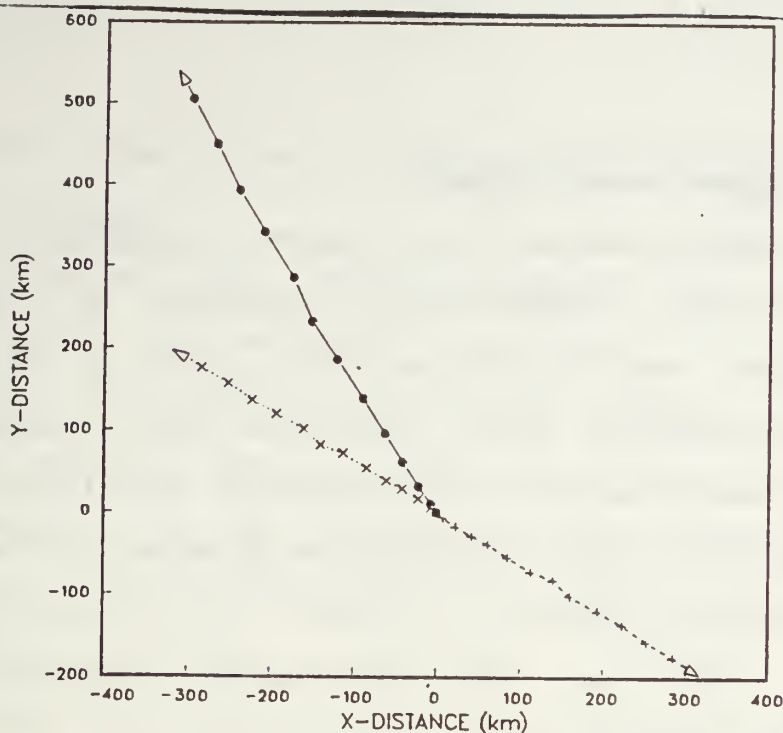


Fig. 17 Vortex tracks each 6 h to 72 h for standard zero mean flow beta effect integration (solid) and positive (dots) and negative (dashed) relative vorticity gradients equal in magnitude to beta on a  $f$ -plane (Williams and Chan 1991).

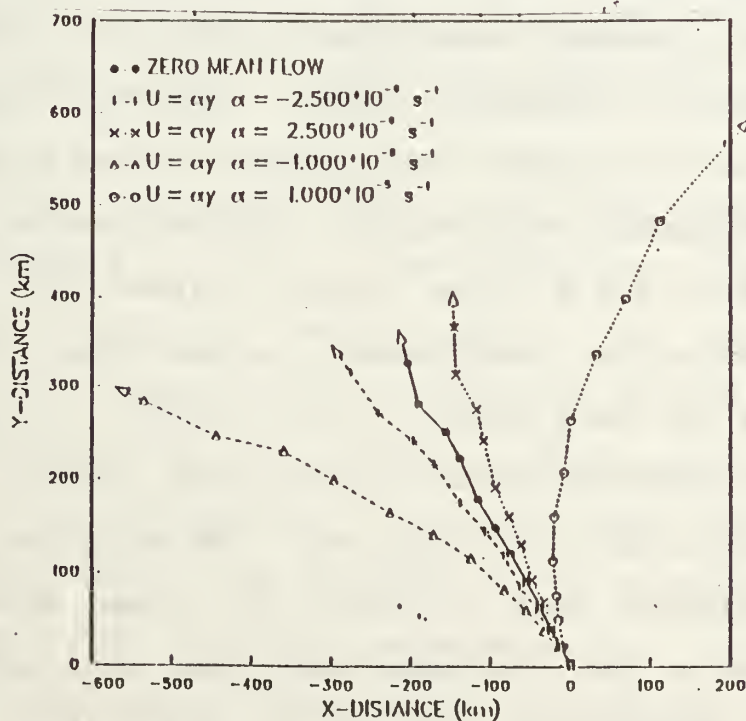


Fig. 18 Tracks predicted by a nondivergent numerical model on a beta-plane with various linearly sheared zonal currents (see legend) (Chan and Williams 1989).

b. Linear shear effect

Interpretation of the above simulations is complicated because both the relative vorticity gradient and the shear effect are included. Notice that the last term in (1) is the advection by the environmental wind of both the vortex vorticity and the vorticity associated with the asymmetric circulation. Willoughby (1979) indicated that wavenumber two asymmetries are generated by the interaction between the vortex and a sheared environmental current. That is, the differential advection due to a meridionally sheared zonal current will lead to a checkerboard pattern of vorticity tendencies in the four quadrants as it acts on the radial gradient of vorticity in the symmetric vortex. Although wavenumber two gyres are produced, no effect on vortex motion occurs because these gyres do not have a flow between them that advects the symmetric vortex. However, the sheared zonal current also will distort the asymmetric gyres and thus modify or produce wavenumber one gyres that do affect vortex motion.

Chan and Williams (1989) included only a linear zonal wind variation that contributes via term four in (1), but does not add to the beta effect in term three. In general, a more westward (northward) track resulted from cyclonic (anticyclonic) shear of the zonal wind (Fig. 18). The analytical model of Carr (1989) indicates that inclusion of linear shear rotates the orientation of the wavenumber one gyres in a manner consistent with the propagation changes in Fig. 18. However, the significant track curvatures in Fig. 18 suggest that some non-

steady process also is contributing to the absolute vorticity propagation process.

Ulrich and Smith (1991) illustrate that a linear wind shear strengthens the wavenumber one gyres, but increases the offset of the gyre axis from the vortex center. For positive shear (more westerly component with increasing latitude), the poleward component of the asymmetric flow across the vortex center is only slightly increased, so that the poleward track deflection is increased. Conversely, a negative shear will slightly reduce the poleward deflection due to the beta effect. Even small deflections will lead to east-west track changes (Fig. 18) as the vortex center moves into faster or slower zonal wind regions. The analytical model of Smith (1992) isolates the term that introduces a wavenumber one gyre oriented east-west across the vortex center, which is thus associated with the poleward deflection.

Williams and Chan (1991) show that subtracting the zonal displacements in Fig. 18 associated with these poleward deflections collapses the tracks back to the zero-shear case within about five degrees. This calculation reveals more clearly that the only difference is a larger (slightly smaller) poleward deflection in the anticyclonic (cyclonic) shear case, as Ulrich and Smith (1991) find. The magnitude of the poleward deflection is consistent with stronger wavenumber one gyres in the anticyclonic shear case. The Fourier analysis by Williams and Chan (1991) indicates the phase of the wavenumber two contribution remains near  $45^\circ$  due to the opposing advection

tendencies of the anticyclonic environmental flow and the vortex circulation, so that the amplitude of the wavenumber one gyres continues to grow. Since the cyclonic shear and cyclonic vortex effects act in the same sense, wavenumber two comes into phase with the forcing and the contribution to the growth of wavenumber two ceases.

c. Potential vorticity effect due to layer thickness

Willoughby (1991) addresses the potential vorticity gradient effect that appears in term three of (1) for a shallow-water model with north-south gradients in layer thickness associated with a uniform basic current. Unless a very shallow layer is assumed, this effect will be negligible compared to the absolute vorticity gradient. Such a potential vorticity gradient will cause an outward (inward) deflection of the vortex that is embedded in a large-scale anticyclonic (cyclonic). Although Ulrich and Smith (1991) show similar deflections, their small domain probably distorts the wavenumber one gyres after only a day.

In summary, the contribution of the environmental shear in distorting the effect due to the relative vorticity gradient is not well understood. The combined effect appears to be time-dependent and may be difficult to diagnose.



## 6. Adjacent synoptic and mesoscale circulations

In the previous section, the environmental shear and vorticity generally were oriented in one direction with little variation along the perpendicular direction. That is, the environmental variations were on large scales compared to the tropical cyclone. In this section, the environment is considered to include adjacent synoptic and mesoscale circulations with scales comparable to the tropical cyclone.

### a. Binary cyclones

The literature on interaction of two tropical cyclones dates back to Fujiwhara (1923). Theoretical studies in the 1940s through the 1960s are summarized in Khandekar and Rao (1971), who used a multiple point-vortex approach to simulate some modifications to the binary cyclonic rotation of Fujiwhara. Chang (1983) re-opened the question with a 3-d numerical simulation that seemed to suggest that the convergence associated with the cyclones must be responsible for the mutual attraction of the vortex pair.

DeMaria and Chan (1984) applied the vortex outer wind structure concepts in Section 3 to argue that attraction/repulsion could be due to the vorticity gradient of one vortex acting as the "environment" of the second vortex. That is, the radial vorticity gradient of two large vortices could be negative at a separation distance of 500 km, and positive if the vortices are small. Using the same reasoning as above for the beta effect, the advection of this negative (positive) vorticity gradient by the symmetric vortex circulation would lead to an

attraction (repulsion) for large (small) vortices. Although DeMaria and Chan confirm this hypothesis with a nondivergent barotropic model, this does not preclude possible contributions by convergent motions associated with tropical cyclone convection. This study does illustrate how an adjacent synoptic-scale circulation can contribute to the environmental vorticity gradient that affects vortex motion in a nondivergent, barotropic model.

Smith et al. (1990) simulate a binary interaction of a strong vortex and a weaker vortex 400 km to the east. The weaker vortex suffers a rapid distortion due to the tangential wind shear of the stronger one (Fig. 19), as would be expected from the Carr and Williams (1989) barotropic stabilization process. The vorticity associated with the weaker vortex is only an elongated vortex filament after 24 h (Fig. 19b) because the radial shear of the angular velocity is large at this distance from the center of the larger vortex. If this vortex had been placed at a greater distance from the center where the radial shear is smaller, the distortion would not have been so rapid. Whereas the weaker vortex is swept cyclonically around the stronger vortex, the influence on the track of the stronger vortex is small. Smith et al. attribute this southeastward displacement to the cyclonic wind distribution of the weaker vortex and the asymmetric vorticity distribution that is associated with the remains of the weaker vortex (Fig. 19c for an  $f$ -plane and Fig. 19d for a beta-plane).

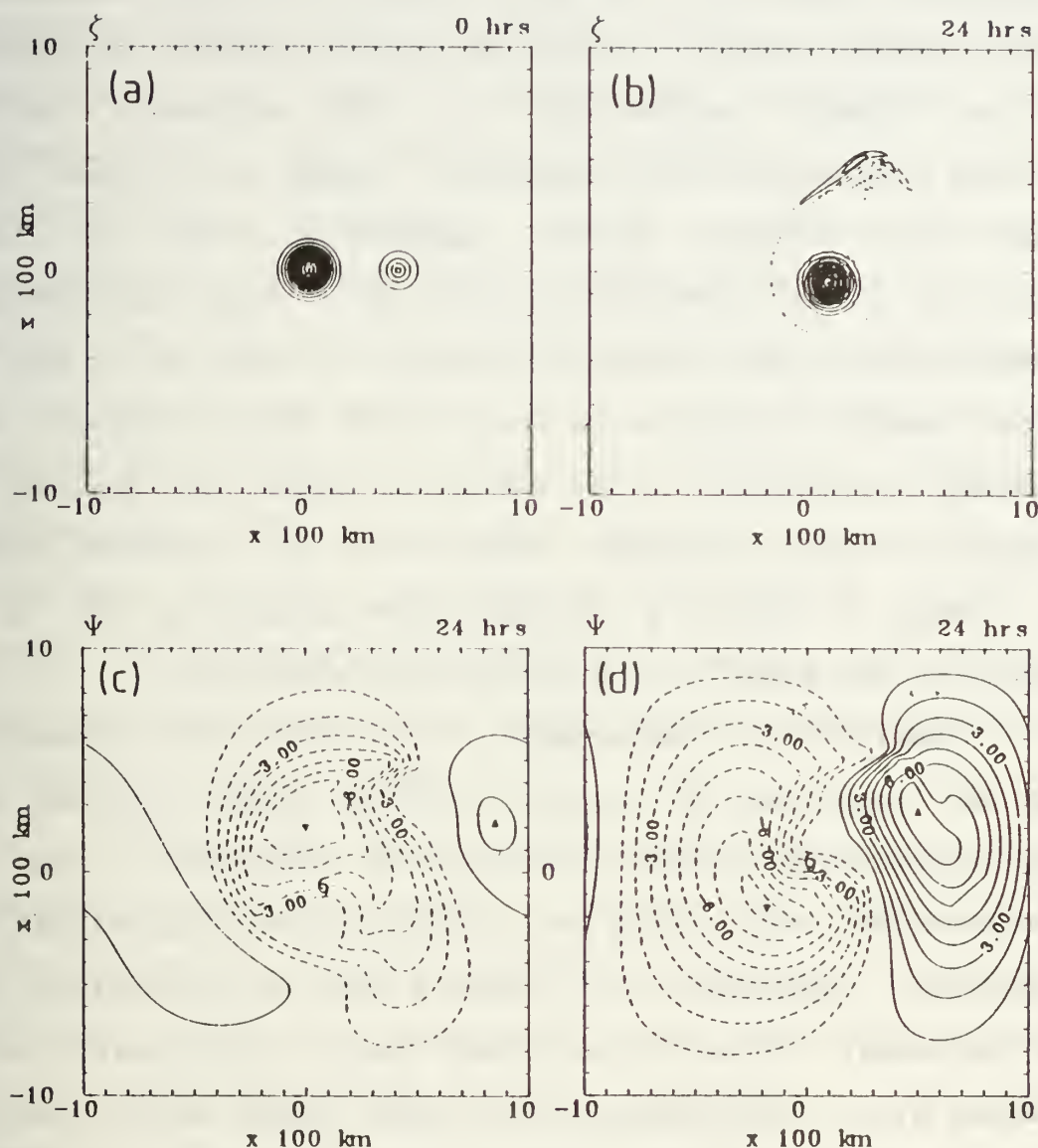


Fig. 19 Relative vorticity fields (a) at the initial instant and (b) at 24 hours in the case of strong vortex, weak-vortex interaction on an  $f$ -plane. The contour interval is  $1.0 \times 10^{-4} \text{ s}^{-1}$ . Shown in (c) is the corresponding environmental streamfunction field at 24 hours, 'environmental' being defined relative to the large vortex. (d) Shows the same streamfunction field for the case of the vortices interacting on a beta-plane. Contour intervals in (c) and (d) are  $10^5 \text{ m}^2 \text{ s}^{-1}$ . Zero contours have been excluded (Smith et al. 1990).

Holland and Lander (1991) have hypothesized that the medium-scale (amplitude  $> 50$  km and period  $> 1$  day) meanders in tropical cyclone tracks are due to synoptic-scale interactions (such as binary interaction) or with mesoscale vortices associated with convective complexes. Lander and Holland (1991) document the complex tracks associated with 10 binary interactions in the western North Pacific. Some cases ended by the destruction of one vortex by the other vortex as in Fig. 19. In other cases, the period of relatively stable cyclonic orbit was rapidly terminated (termed escape by Lander and Holland) and the cyclone tracks diverged relative to the midpoint between them. Cases of escaping cyclones were frequently due to the influence of the shear in the midlatitude westerlies.

Holland and Dietachmeyer (1991) study the interaction, merger and repelling of tropical cyclone scale vortices using contour dynamics and numerical modelling techniques. They show that escape may result from nonlinear processes associated with the vortices. Holland (1991) showed a case of interaction among three vortices. One vortex first moved cyclonically as it interacted with a near-neighbor, but then curved anticyclonically due to a jet-like flow between the wavenumber one gyres associated with the vortices. Such a triple tropical cyclone interaction among tropical cyclones Pat, Ruby and Odessa during 1985 is shown by Lander and Holland (1991). Thus, these numerical studies appear to address some of the complex interactions and resulting track meanders associated with adjacent synoptic-scale cyclones.



b. Mesoscale circulations

Willoughby (1988, 1991) has modelled asymmetric convective forcing in a tropical cyclone as a rotating mass source-sink pair that is located just outside the radius of maximum winds. The convection is assumed to have a wavenumber one distribution in azimuth. If the convection rotates around the center with the average wind speed at that radius, the vortex center also has a circular motion with the same rotation rate. If the vortex is embedded in an environmental current, the combined motion effect is a cycloidal track (Fig. 20a) similar to observations. Willoughby (1991) shows that the flow between an inner pair of gyres contributed to advection of the vortex center. When the mass source-sink is removed after 18 h, these gyres are dissipated by the radial shear and the circular motion of the vortex center stops.

Willoughby (1991) also treats the case of a non-rotating convective center. Because this mass source-sink maintains the same orientation with respect to the center, quasi-stationary gyres are established that persistently advect the vortex center toward the enhanced convection. The interesting aspect of this case is that this non-rotating forcing caused a normal mode response associated with the larger scale gyres. Thus, the deflection toward the side where the asymmetric convection occurs continues after the mass source-sink is removed (Fig. 20b). This result suggests that initial asymmetries that project onto the normal modes could sustain persistent

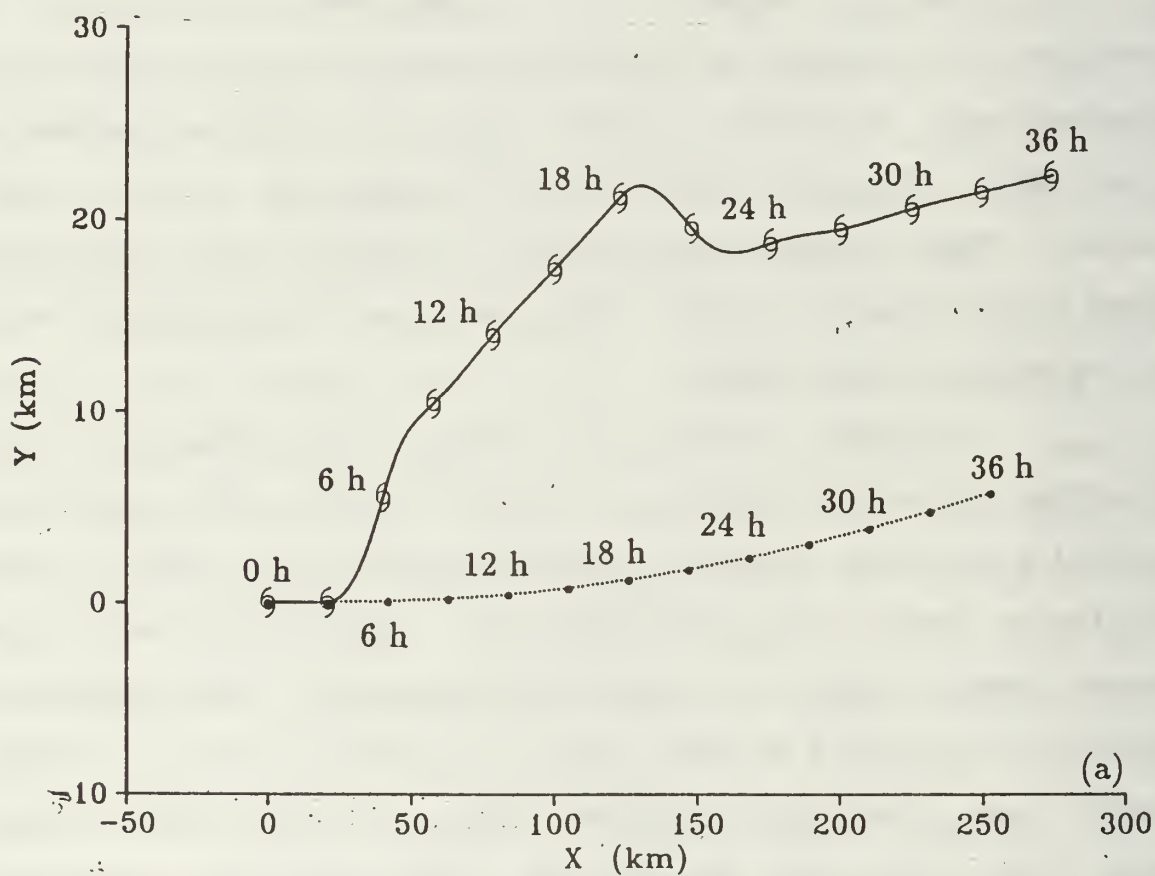
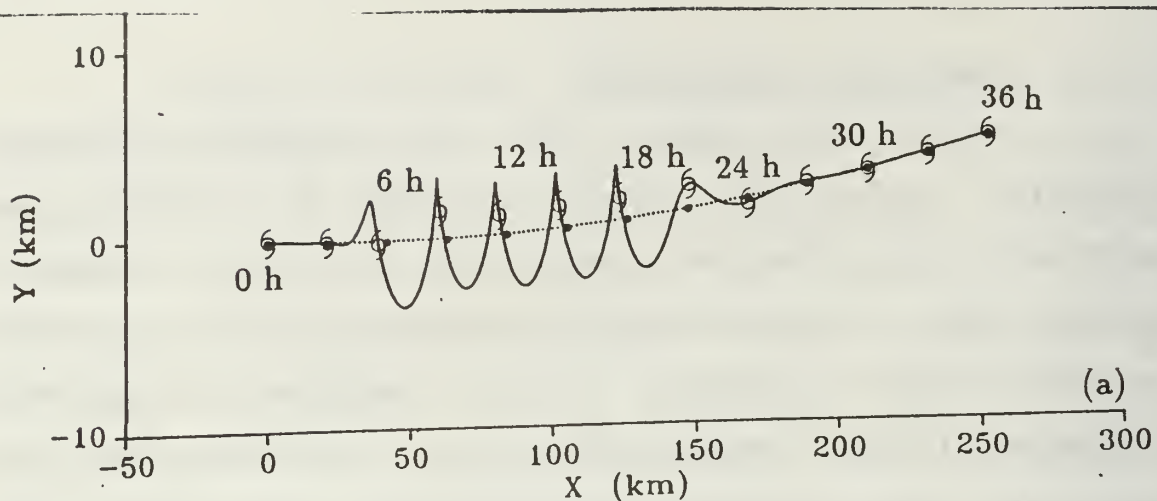


Fig. 20 Vortex tracks (solid) with (a) rotating and (b) non-rotating mass source-sink just outside the radius of maximum winds and embedded in a  $2 \text{ m s}^{-1}$  westerly basic current. The source-sink is started at 3 h and stopped after 18 h. The dotted line indicated the vortex track without the mass source-sink. Notice the ordinate scale is much smaller than the abscissa (Willoughby 1991).

deflections relative to environmental flow even after the forcing or initial asymmetries are removed.

Holland and Lander (1991), Lander and Holland (1991) and Holland and Dietachmayer (1991) suggest that the mesoscale vortices that develop in an active monsoon trough may interact among themselves (perhaps to form a tropical cyclone) and with an existing tropical cyclone. Satellite imagery occasionally reveals a major mesoscale convective complex on the periphery of a tropical cyclone. If a mesoscale vortex is associated with this convective complex, the same vorticity dynamics should apply. The tendency will be for the radial shear of the symmetric vortex circulation to distort the mesoscale vortex as in Fig. 19. However, strong convection may sustain the mesoscale vortex against dispersion. Consequently, a significant track deflection might occur as in the non-rotating mass source-sink experiment (Fig. 20b) of Willoughby (1991). A demonstration of this effect in nature and an improved understanding of the process could contribute to better forecasts when such track meanders are present.

## 7. Implications of barotropic model studies

Before discussing recent baroclinic model studies of tropical cyclone motion, some discussion of the barotropic model results is appropriate. Some preliminary attempts have been made to validate the barotropic interpretations using available tropical cyclone data sets. In addition, the experimental design of the Tropical Cyclone Motion (TCM-90) field experiment during August-September 1990 was based in part on these ideas.

### a. Wind field decomposition

First, consider the definition of the problem in terms of a three-component decomposition of the total wind field into a symmetric vortex, a large-scale environmental current and an asymmetric circulation that arises due to the nonlinear interaction between the vortex and the environment. Implied in this definition is the concept that the departure of tropical cyclone motion relative to the environmental current is due to a basic process called propagation. Carr (1989) refers to a "self-advection" that combines the linear and nonlinear processes into a single propagation vector (see Section 3a). That is, the basic vortex circulation creates a specific asymmetric circulation depending on whether the forcing is due to the beta effect, the environmental relative vorticity gradient, a mass source-sink pair representing asymmetric convection, etc.

The tangential wind profile of the vortex has an essential role in the forcing process and in the adjustment to that forcing. The outer wind profile is critical in the beta effect (or absolute vorticity gradient) forcing of the gyres (see



Section 4). The radial gradient of the vortex angular velocity leads to barotropic stabilization that tends to eliminate azimuthal waves and maintain axisymmetry. In particular, an inner core region of 300-500 km radius exists in which the asymmetric vorticity is homogenized. Thus, a nearly uniform region of flow between the pair of counterrotating gyres is created (see Section 3b). The advection of the basic vortex within this nearly uniform flow is the propagation vector. As indicated above, the character of the asymmetric circulation can vary depending on the forcing, but the basic physical processes that adjust the asymmetric circulation is a self-advection mechanism. The normal mode interpretation of Willoughby (1990, 1991) is useful in understanding the asymmetric circulation response to the forcing. Regardless of the forcing or the environmental shear distortions, this inner core region remains and the relative motion with respect to the vortex center is near zero. That is, the vortex center propagates with the uniform flow region.

An alternate definition, and interpretation of the physical processes, has been advocated by Professor Roger Smith. Following Kasahara and Platzman (1963), Smith considers a two-component system of a fixed symmetric vortex and an environment that contains the large-scale flow, the asymmetric circulation induced by the forcing and adjustment process described above, plus the time changes in symmetric forcing. Rather than use the term "propagation", which implies a different physical process, Smith emphasizes that the advection by the asymmetric circulation

is a similar process to the advection by the large-scale flow. Smith thus advocates combining both into the definition of the environment, and the total motion of the vortex is thus due to advection by this environment. Indeed, numerical models and some recent observational studies by HRD-NOAA (Roux and Marks 1991) indicate the vortex moves with the integrated flow over some small domain near the center.

Some disadvantages of the two-component decomposition can be given. First, the vortex circulation is continually changing as the tropical cyclone develops and decays. Furthermore, the basic barotropic stabilization process of Carr and Williams (1989) involves an inward angular momentum flux that accelerates the inner winds and creates anticyclonic winds on the outside. These wind profile changes cause dramatic oscillations in the integrated relative angular momentum (RAM) for a completely cyclonic initial vortex. Since the propagation effect (or the term "relative motion" preferred by Smith) depends on the outer wind structure, the time-dependent character of the vortex can not be ignored. Whereas it is convenient to maintain a fixed symmetric vortex in theoretical studies, this does not apply in nature and the vortex changes should not be included in the definition of the environment. In addition to making observational verification impossible, such a definition obscures the physical processes that need to be understood.

The advantage of separating the asymmetric circulations from the definition of the environment is that specific structures can be sought in the observations to validate

different mechanisms that contribute to tropical cyclone motion. In addition to being drawn to the simplicity and theoretical convenience of the Kasahara and Platzman decomposition, Smith evidently believes it is impossible to detect the asymmetric circulations in observational data sets (see below). The numerical model outputs have adequate horizontal resolution and accuracy to document the structure and evolution of these wavenumber one gyres and the symmetric vortex changes. In general, the data coverage in the tropics is inadequate to detect such structures and their changes. However, the key point is that the analytical and numerical model studies provide a detailed specification of these structures. Knowing the shape, amplitude, orientation, etc. of a signal makes design of an observational system and an analysis technique to detect that signal from a sparse data set a more viable endeavor.

Another practical problem in the wind decomposition is the definition of the steering. As indicated in Section 2, the radial-band averages of the wind field should remove the symmetric vortex. However, Carr and Elsberry (1991) argue that radial-band averages will also include a contribution from the circulation in Fig. 6 because the gyres are not symmetrical relative to the storm center. They demonstrate that radial-band averages for the gyres that would be expected due to only the earth vorticity gradient in a non-divergent barotropic model of tropical cyclone motion would lead to a rotation and decreased amplitude of the steering vector similar in form to Fig. 1. Because the Carr and Elsberry gyres were generated with a model



that had no environmental flow, the radial-band averages were entirely due to the asymmetric circulation.

Regardless of whether the gyres in Fig. 6 are due to barotropic processes or other physical mechanisms, a component from these asymmetric gyres will be included as part of the steering flow calculation of the radial-band averages. Subtraction of this false steering from the storm motion will then distort the calculation of the propagation vector. That is, the radial-band method of calculation does not define a unique decomposition into the steering flow. Some method must be developed that eliminates both the symmetric and asymmetrical circulation (Fig. 6) components and leaves only the large-scale environmental flow that represents the steering flow in the wind decomposition.

b. Detectability of gyres from observations

Reeder et al. (1991) use an asymmetric circulation pattern similar to Fig. 6 for a quiescent environment to assess the ability of a static objective analysis technique to detect such gyres. In addition to the visual comparisons of patterns, Reeder et al. compare point estimates of speed and direction of the flow-through between the gyres at the center of the storm. Such point estimates are likely to be affected by small-scale disturbances in the fields. The sensitivity to the analysis scheme filtering characteristics is first tested with the full 10 km resolution of the original data set. The resulting smoothing of the symmetric circulation introduces a large erroneous component into the derived asymmetric circulation



calculated with the Kasahara and Platzman technique of subtracting the initial symmetric circulation. This is another example of the inappropriateness of using the Kasahara and Platzman technique with analyzed data. When the azimuthal average of the smoothed symmetric circulation is used in the decomposition, the speed and direction of the asymmetric circulation at the center are retrieved well.

Reeder et al. then assess the required data coverage to resolve the gyres by degrading the model data set to 50, 100, 150 and 200 km resolution. They also test the island rawinsonde distribution for TCM-90 to determine whether that data set will be adequate. They conclude that 100 km resolution will be required in the data set, which is not surprising in view of the 1000 km scale of the gyres. They also conclude that (their version of) the TCM-90 network is inadequate to resolve the gyres satisfactorily.

In a forthcoming comment, Holland et al. (1991) disagree with the Reeder et al. (1991) conclusions. First, Holland et al. use an objective analysis scheme that filters only the increments, which avoids the over-smoothing of the full field that resulted in the Reeder et al. technique. Neither of these approaches makes use of the time continuity in the fields that is one of the advantages of the four-dimensional data assimilation technique used at most analysis and forecasting centers. Holland et al. use a larger vortex that is more representative of typical typhoons than the small vortex that Reeder et al. had to use due to the small domain of their numerical model. Consequently,

their asymmetric circulation has larger amplitudes and horizontal scales than that of Reeder et al. Finally, Holland et al. include the adjacent land stations over the Asian continent and representative lower tropospheric cloud-drift wind sets that are part of the TCM-90 data set. Neither group includes the commercial aircraft reports, surface reports or the Tiros operational vertical sounder profiles that also will be in the TCM-90 data set. Nevertheless, the observational density in the Holland et al. study is about 10 times the coverage of Reeder et al.

Holland et al. demonstrate that inclusion of only the upper-air soundings is sufficient to reproduce the major features of the model-simulated gyres. Inclusion of the cloud-drift winds allows their analysis scheme to reproduce the major asymmetries almost exactly. In contrast to Reeder et al., Holland et al. conclude that their more representative TCM-90 data distribution would be capable of analyzing a realistic wavenumber one gyre pattern for a quiescent environment.

The analyses of the environment of hurricane Josephine as it developed over a 3-day period were examined by Franklin (1991) for evidence of an asymmetric environment (Fig. 21). On the first day, Josephine was a strong tropical storm ( $31 \text{ m s}^{-1}$ ) with an asymmetric convection distribution, and a frontal trough was present to the northeast of the storm. The derived asymmetric circulation on this day has a wavenumber two circulation more characteristic of a sheared environment (Fig. 21a). By the last day, a cyclonic gyre seems to be developing

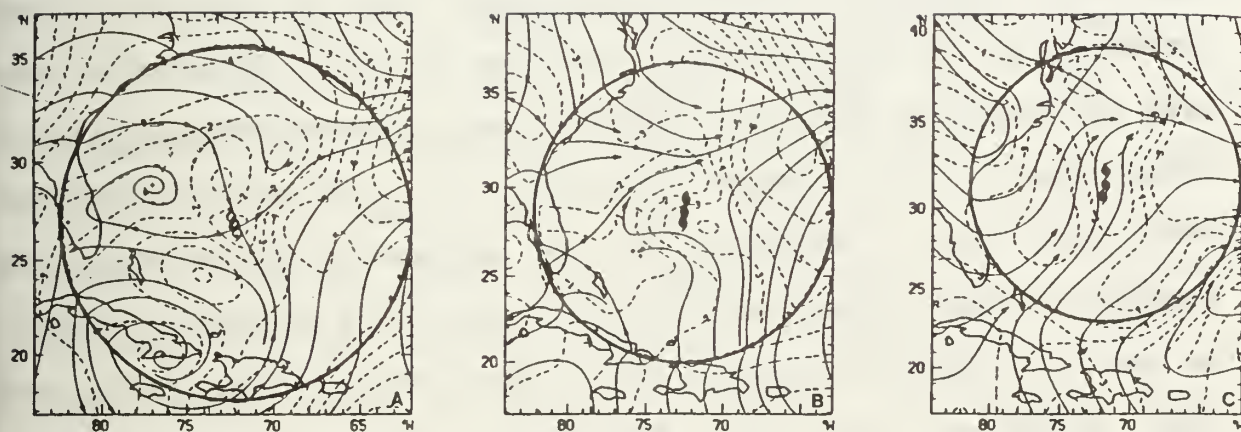


Fig. 21 The 300-850 mb mean environmental wind field for 10/00 (a), 11/00 (b), and 12/00 (c) determined by subtracting the symmetric component (azimuthal mean vortex) from the total wind. Outside of the radius of the nearest domain boundary (heavy circle), the total wind field is shown. The contour interval for the isotachs is  $1 \text{ m s}^{-1}$ . Josephine's positions at 6-h intervals are indicated by the tropical storm/hurricane symbols; the center symbol indicates the 0000 UTC position (Franklin 1990).

about  $8^\circ$  long. to the west-northwest of Josephine (Fig. 21c). Although no closed anticyclonic center is observed to the east, the flow-through in the region of the storm is consistent with the storm path.

Kaplan and Franklin (1991) have attempted to isolate the asymmetric circulation associated with tropical storm Florence using a special data set of dropwindsondes over the Gulf of Mexico and surrounding rawinsondes. Although the wavenumber one gyres should be weak at this storm stage, some evidence of the gyres appear in their analysis.

c. Validation of absolute vorticity gradient dependency

As indicated in Section 5, some disagreement exists regarding whether a simple relationship between propagation and the local absolute vorticity gradient can be proved. The introduction of environmental relative vorticity gradients does make the absolute vorticity gradient the relevant variable in the third term in (1). However, the shear in such an environmental wind field also contributes to the asymmetric circulation via shearing of the wavenumber one gyres and of the symmetric vortex. As noted by several authors (e.g., Chan and Williams 1989; Carr 1989; Ulrich and Smith 1991; Williams and Chan 1991), the effect of linear anticyclonic shear is not just the opposite of a linear cyclonic shear. Smith (1991) found that the inner shear distortion of the symmetric vortex vorticity can lead to a wavenumber one contribution that has a meridional advective component across the vortex center. Evans et al. (1991) note that the modification of the environment by the vortex will also



change the relationship between propagation and the absolute vorticity gradient.

Carr and Elsberry (1990) argue that the rotation of the propagation vector direction from west-southwestward for westward moving cyclones (Fig. 2b) is consistent with absolute vorticity gradient differences. Both north-south and east-west vorticity gradients in the environment must be considered in the western North Pacific when a cyclonic circulation associated with the summer monsoon is present. Evans et al. (1991) use climatological wind fields in this region to illustrate the spatial variability that might be expected in the propagation. The short-term changes in propagation for initial positions poleward and equatorward of the subtropical anticyclone in barotropic models (DeMaria 1985; Shapiro and Ooyama 1990; Evans et al. 1991) seems to support the absolute vorticity dependence.

Smith and Ulrich (1991) argue that the vortex asymmetries do not achieve a steady configuration, but continue to evolve on a time scale of days. They make these conclusions based on numerical model integrations started with no asymmetric circulations, and the time required for the gyres to achieve a quasi-steady state is 24-48 h (Fiorino and Elsberry 1989a). Storms in nature would have continually evolving asymmetric circulations as they develop and move into regions of changed environmental vorticity gradients.

Willoughby (1991) also suggests that the asymmetric circulations may depend on the time history of the forcing rather than the present forcing distribution, e.g., the local absolute

vorticity gradient. If so, the asymmetric circulation will be a balance between the asymmetry-generating mechanisms and the asymmetry-distorting effects.

Some preliminary confirmations of the absolute vorticity gradient dependency are provided by Franklin (1990) and Kaplan and Franklin (1991). The vorticity gradient was estimated from a  $5-7^{\circ}$  lat. radial-band average and compared with the corresponding propagation vectors (Table 3). In general, the comparisons for five cases are fairly consistent and seem to support a linear relationship. Kaplan and Franklin point out that all of these storms were moving within  $20^{\circ}$  of North and thus do not represent a broad spectrum of cases.

d. Initialization of dynamical track prediction models

A common problem in numerical predictions of tropical cyclone tracks is the definition of the initial conditions. Inadequate observations are available to define the symmetric vortex or the asymmetric circulation. It is also difficult to extract the effects of the vortex to define the environmental flow. Many dynamical models have relatively large forecast errors during the first day, but then rapidly improve with time (Elsberry et al. 1987).

Carr and Elsberry (1991) propose that an initial slow bias in such numerical models may be due to insertion of only the symmetric vortex structure, which therefore omits the propagation that would be associated with the asymmetric circulation. That is, the propagation will be missing or underestimated during the 24-48 h period while the model develops

Table 3 Headings (deg.) and magnitudes of the absolute vorticity gradient  $\nabla(f + \zeta)$  and the propagation vector  $V_p$  calculated for the 5-7° lat. radial band within the 850-300 mb layer, except for the Florence (F) case, which is for the 850-500 mb layer. Debby (D) and Josephine (J) are the other hurricanes. Dates are specified as month/day/year and all cases are at 00 UTC (Kaplan and Franklin 1991).

Storm	Date	$\nabla(f + \zeta)$ ( $10^{-11} \text{ m}^{-1} \text{ s}^{-1}$ )	$V_p$ ( $\text{m s}^{-1}$ )
D	9/16/82	353/6.2	003/6.9
J	10/10/84	001/1.8	289/1.8
J	11/11/84	354/2.5	319/2.4
J	10/12/84	351/3.7	317/3.7
F	9/9/88	035/4.8	012/2.7

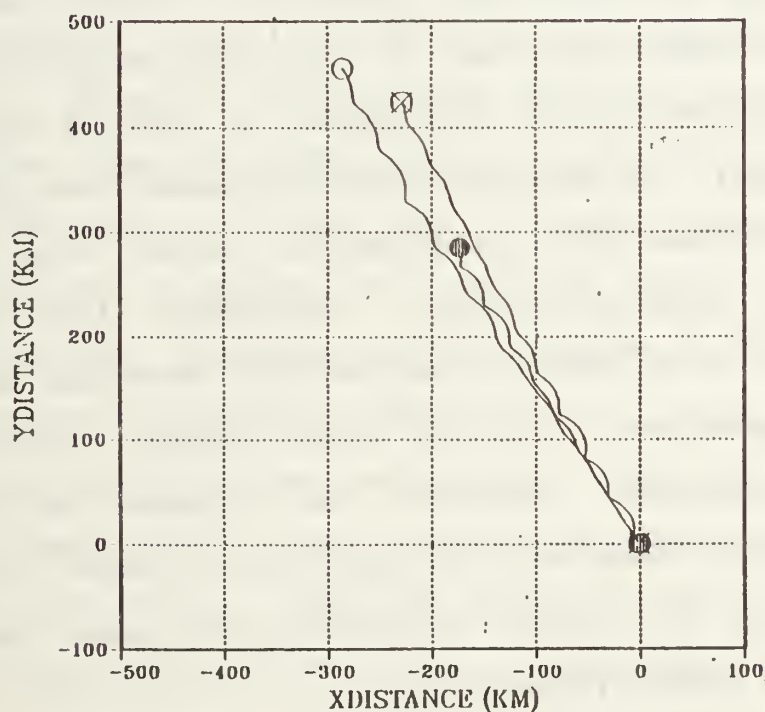


Fig. 22 Tracks predicted by Chan and Williams (1987) numerical model for: symmetric initial vortex, 0-48 h (solid circle); symmetric initial vortex, 36-84 h repositioned to same starting point (crossed circle); and asymmetric initial vortex including wavenumber one gyre, 0-48 h (open circle) (Carr 1989).

the appropriate gyres. Carr and Elsberry illustrate the effect with a nondivergent, barotropic model forced by beta only. Rather than starting with no asymmetric circulation, they use the Carr (1989) analytical model to define the appropriate wavenumber one gyres for the initial symmetric vortex. The Carr model has an internally derived propagation vector, or this propagation can be externally specified. In either case, the inclusion of the wavenumber one gyres produces immediately an essentially steady propagation. The along-track error at 48 h was reduced from greater than 150 km to less than 60 km (Fig. 22).

Each of the other analytical models by Willoughby (1988, 1990, 1991), Smith and Ulrich (1990) or Smith (1991), and Peng and Williams (1991) also could be used to initialize the dynamical model. In each case, the wavenumber one gyres could be specified for the specific symmetric vortex wind profile and environmental wind conditions. Willoughby (1991) argues that specification of a  $RAM=0$  vortex has the advantage of minimizing the Rossby wave radiation that might interact unfavorably with the model boundaries. However, real tropical cyclones are not likely to have a structure corresponding to  $RAM=0$ , and it may be more important to include realistic outer wind structures to introduce the proper propagation.

It is emphasized that such an operational application requires specification of two of the three vectors (propagation, environmental flow and the total storm motion). A key difficulty is to define the environmental flow by removing the effects associated with the vortex. Carr and Elsberry (1991) suggest



some approaches for operational application. As indicated in Section 7a, Carr and Elsberry (1991) demonstrate that the  $5-7^{\circ}$  lat. radial-band average of the total wind field is not an appropriate method for defining the environmental flow, because such averages include a component from the wavenumber one gyres associated with propagation. Smith et al. (1990) and Ulrich and Smith (1991) also use numerical model simulations to illustrate that these radial-band averages do not represent the storm motion because of the wavenumber one gyre contamination.

Mathur (1991) has combined the problems of specification of the initial environmental flow and the inclusion of a propagation vector into one step. His generalized dipole is specified to produce a uniform flow with the same direction and speed as the observed storm vector, rather than being directed along the propagation vector with a uniform flow of  $1-3 \text{ ms}^{-1}$ . The alternative suggested by Carr and Elsberry (1991) is a decomposition that separates the environmental flow problem from the asymmetric circulation calculation. Since the specified asymmetric circulation may persist for some time in the model, some care needs to be taken to derive an appropriate asymmetric circulation for use in dynamical track prediction models. The four analytical models provide the necessary specification.

## 8. Baroclinic effects

As 3-d models were developed to predict tropical cyclone formation and tracks, some idealized simulations were made to test the effect of vertical shear. For example, Madala and Piacsek (1975) found that the vortex moved more rapidly to the north when it was embedded in a basic current with increasing easterlies with elevation. Talbert (1987) also found a rightward deflection relative to the environmental shear vector. An environment with vertical shear may also cause a tilt to develop between the lower cyclonic center and the upper anticyclonic center. Mutual advection associated with such tilted centers may then cause track deflections.

Recent baroclinic models with idealized conditions to understand the effects of vertical structure and vertical shear on tropical cyclone motion will be reviewed first. Inclusion of diabatic heating and friction in these models adds additional complications, but eventually must be done if real cyclones are to be studied. In particular, diabatic heating and momentum mixing are essential mechanisms for vertical coupling of the layers. Because asymmetries in diabatic heating and in friction also contribute to motion, separation of the various contributions becomes difficult. Some recent studies using full-physics, baroclinic models with real data to understand tropical cyclone motion will be reviewed briefly.

### a. Vertical structure models

One purpose for using a baroclinic model is to compare the motion response among the different layers when the cyclone

has vertical structure. Considering the role of the outer wind profile in the barotropic models (see Section 4) with only the beta effect, the different layers in the cyclone would be expected to propagate in different directions. Wang and Li (1991) conducted such an experiment with a 10-level model. An idealized initial tangential wind profile that had a maximum at 900 mb and decreased linearly to zero at 100 mb was specified (Fig. 23). The radial variation (not shown) had a maximum at 200 km and decreased to zero at 750 km, so the RAM integrated over this domain was positive and had a vertical variation similar to the tangential wind structure (Fig. 23). The numerical model was integrated from these initial conditions with the beta effect included, but with no heating or friction. Nevertheless, the vortex maintained vertical coherence as indicated by the essentially constant meridional propagation at all levels indicated in Fig. 23. That is, the vortex circulation remains vertically coupled by the secondary circulation between layers and propagates with the vertical mean of the RAM, just as would be expected in a barotropic model initialized with the vertically-integrated vortex wind structure. While this was true when the vortex was cyclonic at all levels as in Fig. 23, a structure with an anticyclone vortex above did not remain vertically coupled. The anti-cyclonic portion moved west-southwest while the cyclone part moved north-northwest. This separation is due to the lack of a vertical coupling mechanism associated with the tropical cyclone secondary circulation, which is driven by air-sea fluxes in the boundary layer and the heating

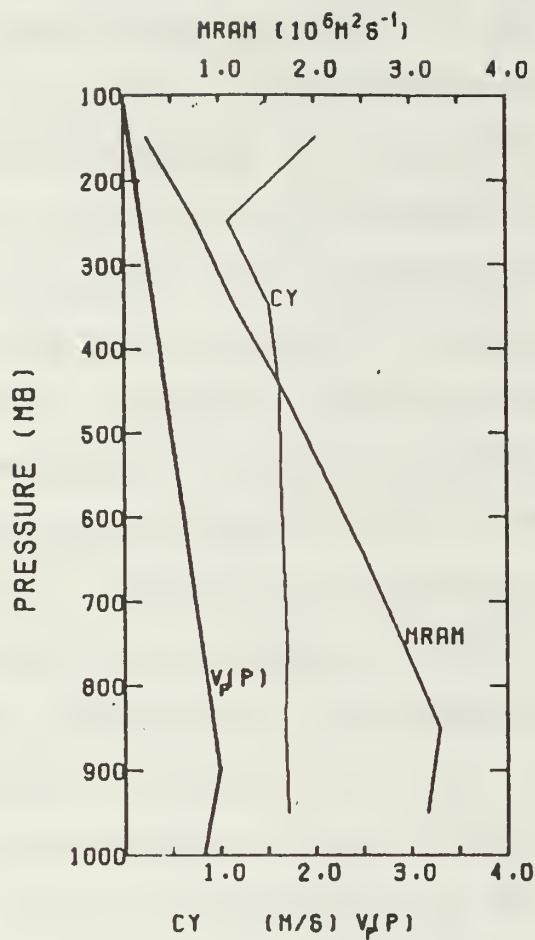


Fig. 23 Initial tangential wind  $V_p$  (normalized by maximum wind) and mean relative angular momentum (MRAM) variations with pressure in the Wang and Li (1991) 10-level numerical model. Mean meridional drift speed  $C_y$  of the vortex at 24 h is also shown.



in the center that ultimately produces the anticyclonic flow aloft. That is, a dry model can not sustain the anticyclone over cyclone structure against the beta effect distortion.

Shapiro (1991) has included simple representations of boundary-layer drag, convective heating and momentum transports in a three-layer model. A tropical cyclone vortex is spun up on a f-plane for 48 h, and then the beta effect is introduced. As in the barotropic models with quiescent flow, the propagation vector is to the north-northwest at about  $2.4 \text{ m s}^{-1}$ . The asymmetric circulation in the middle layer (Fig. 24a) is remarkably similar to the barotropic models such as Fig. 6, with a cyclonic (anticyclonic) gyre to the east (west). These gyres are shown to form from the advection of low potential vorticity (rather than absolute vorticity in barotropic models) from the equatorward side and high potential vorticity from the poleward side (Fig. 24b). Notice also the homogenization of the asymmetric potential vorticity field within about 300 km of the center, as occurred in the barotropic models. In this case, the barotropic stabilization process associated with the radial shear of the angular velocity also is tending to homogenize the asymmetric effects of the convective heating and momentum distributions. Although the flow between the cyclonic-anticyclonic gyre pair is not as uniform as in the barotropic models, it clearly advects the vortex to the north-northwest. Even though Shapiro notes that enhanced convection on the forward side relative to the trailing side could also be contributing,

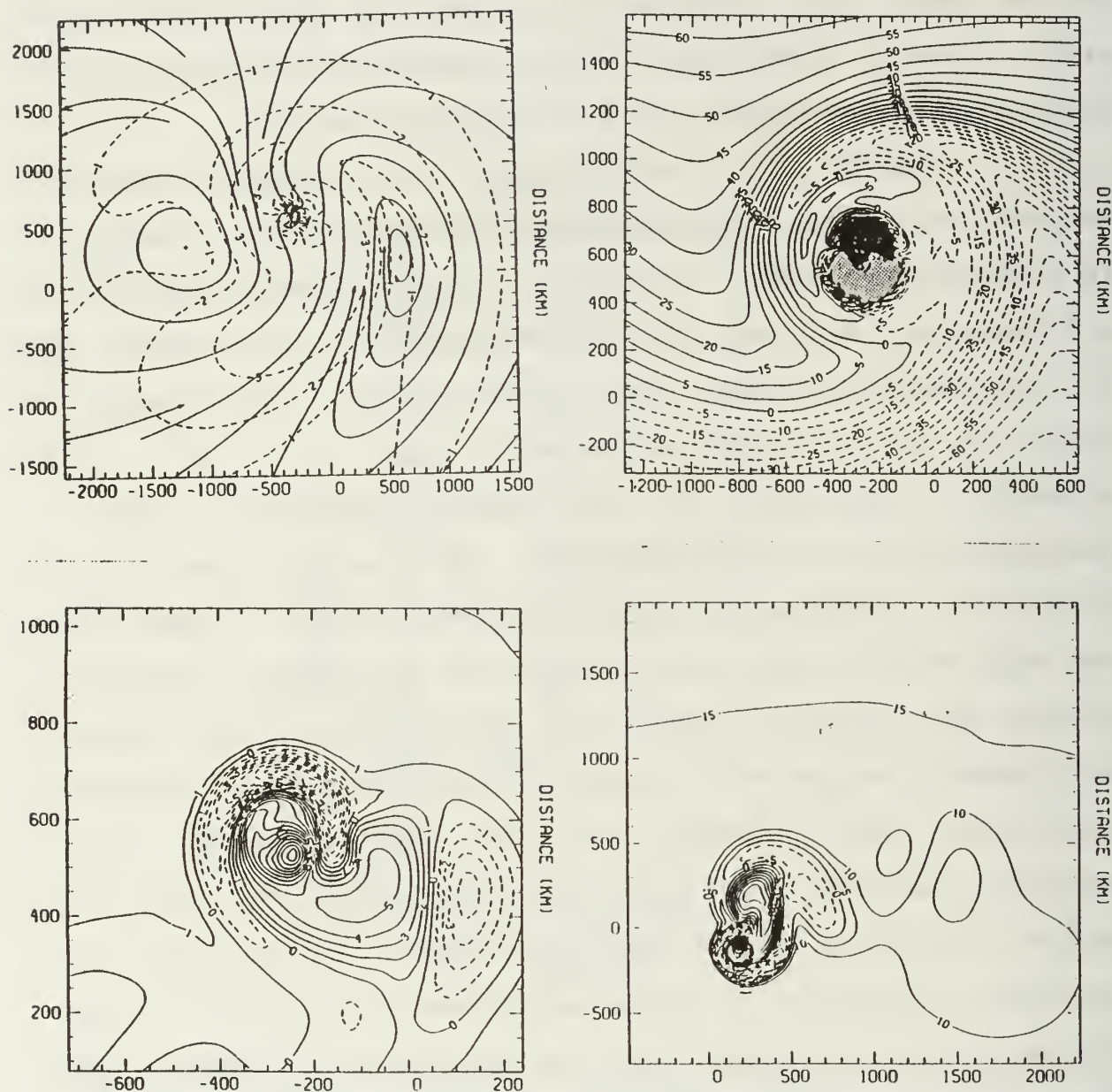


Fig. 24 Asymmetric (a) wind (contour  $1 \text{ m s}^{-1}$ ) and (b) potential vorticity (contour  $5 \times 10^{-10} \text{ m}^{-1} \text{ s}^{-1}$ ), shaded for less than  $-85 \times 10^{-10} \text{ m}^{-1} \text{ s}^{-1}$  at 120 h in middle layer of the Shapiro (1991) baroclinic model for a vortex on a beta plane. (c) Potential vorticity (contour  $1 \times 10^{-10} \text{ m}^{-1} \text{ s}^{-1}$ ) in upper layer near center of vortex with no vertical shear and (d) with westerly shear in upper layer (contour  $5 \times 10^{-10} \text{ m}^{-1} \text{ s}^{-1}$ ).

the association of the propagation with the asymmetric circulation is quite convincing.

The vertical heating distribution creates negative potential vorticity anomalies in the upper layer of the Shapiro model, and the convective momentum flux deposits positive potential vorticity from below. Consequently, the potential vorticity distribution above the center is quite complex (Fig. 24c). A wake of positive and negative anomalies with large magnitudes trails behind the center. On the larger scale, the outer anticyclonic circulation advects high (low) potential vorticity values to the east (west) side of the center, which will tend to create wavenumber one gyres in the upper layer that are in the opposite sense as the gyres in the middle layer. Although the upper-layer gyres tend to advect the vortex toward the south, this effect is small compared to the northward advection by the middle-layer gyres.

The processes that contribute to changes in RAM are more complex in the baroclinic model than in the barotropic model. First, air flowing toward the center at low levels loses angular momentum to the underlying surface, so the total RAM in the volume around the cyclone is decreasing in time. However, the net horizontal momentum flux into the area within 3000 km of the center tends to offset the frictional loss and the RAM becomes constant.

In summary, the baroclinic model results suggest that many of the barotropic model concepts may be applied if a



vertical average that does not include the outflow layer is used to define the vortex structure.

b. Vertical shear effect

A demonstration of the potential effects of vertical shear in tilting the vortex has been provided by Wu and Emanuel (1991). They use a contour dynamics approach involving patches of constant potential vorticity to represent the upper anticyclonic and the lower cyclonic circulations. They simulate the creation of negative potential vorticity above the convective heating region as an expanding patch of negative potential vorticity values. However, they do not include the momentum transport by the convection that maintains a cyclonic outflow region above tropical cyclones. As the upper vortex patch expands and is advected downstream in the vertically sheared flow, the lower vortex drifts meridionally under the influence of the upper-level circulation. Without the convective momentum source to maintain the system in a vertical alignment, the tilt proceeds. Meridional drifts as large as the beta drift are predicted for optimal vertical tilt. The effect is dependent on the ratios of the layer thicknesses and the vortex sizes.

Flatau (1991) also studies the effect of vertical shear in a 3-d model in which the secondary circulation is forced by a specific heat source. This heat source is arbitrarily specified rather than having been diagnosed to maintain the lower cyclonic and upper anticyclonic structure of the vortex. The meridional deflections increase as the tilt increases until the region of maximum anticyclonic flow is directly above the low-level center.



In both of these cases, the mechanisms for maintaining a vertically coherent tropical cyclone are omitted. Whereas the resultant tilted structure would likely produce the magnitude of deflections predicted in these models, no evidence exists for such large tilts in nature. Roux and Martin (1991) suggest the inner core may have been tilted by 5-10 km in hurricane Hugo even though a consistent vertical shear was detected from the surface to 8.5 km. Thus, the processes that maintain the vertical structure limit the tilts and probably lead at most to the oscillatory motions of less than 10 km as described by Khandekar and Rao (1971).

Shapiro (1991) illustrates the effect of vertical shear in a 3-layer model that does include the convective heating and momentum fluxes into the upper layer. To simplify the interpretation, the westerly zonal flow is added only in the upper layer, and beta is set to zero. Because the thermal wind between the middle and upper layer requires larger thickness to the north in the middle layer, the potential vorticity gradient is southward in this layer. Consequently, the motion of the vortex is southward and eastward at an average speed of about  $0.9 \text{ m s}^{-1}$ . That is, the cyclonic vortex now advects low (high) potential vorticity values in the middle layer southward (northward) on the west (east) side of the cyclone. Anticyclonic (cyclonic) gyres form on the west (east) side and the flow between the gyres is to the southeast when beta is zero.

The important contrast with the Flatau (1991) and the Wu and Emanuel (1991) studies is that the system remains almost

vertical even though an upper-level wavenumber one asymmetry is established due to air blown eastward by the environmental wind (Fig. 24d). The low potential vorticity anomaly about 1500 km to the east of the vortex in the upper layer induces an anticyclonic anomaly in the middle layer (not shown) that tends to move the vortex to the north. Shapiro concludes that the northward gradient of potential vorticity in the upper layer has little effect on the vortex motion. By contrast, the southward gradient of potential vorticity is both necessary and sufficient to explain the southeastward drift.

An important consideration in all of the baroclinic models (and probably in nature) is the depth of the upper outflow layer. When Shapiro made the upper (middle) layer shallower (deeper), the southeastward speed on this  $f$ -plane was reduced to about  $0.3 \text{ m s}^{-1}$ . The decrease in propagation was nearly proportional to the reduction in the potential vorticity gradient associated with the greater middle layer depth. As the outflow is confined to a shallower layer, the momentum flux from below will drive a cyclonic flow above the low-level center that will spiral outward and become a stronger anticyclonic flow at large radii. With the northward gradient of potential vorticity in the upper layer, this anticyclonic flow will induce an asymmetric circulation that will produce a northward motion tendency. Thus, the reversal of the upper-layer and middle-layer potential vorticity gradients tend to produce offsetting tendencies due to vertical shear on an  $f$ -plane.

In summary, the baroclinic model of Shapiro (1991) strongly suggests that the basic dynamics of tropical cyclone motion are similar to those derived from barotropic models. That is, the first-order propagation effect is induced by the midtropospheric cyclonic vortex circulation advecting the potential vorticity gradient associated with beta and the relative vorticity gradient. The important structural feature is the depth-averaged cyclonic flow. The role of the convective heating and momentum flux is crucial in maintaining a realistic vertical structure. Gray (1991) has described a baroclinic environment effect that is observed as a relative vorticity gradient toward the left of the track. A northwest propagation is hypothesized if the beta effect and asymmetric convection on the south side are included. Present indications are that effects of asymmetries in heating and friction are smaller than the effects of the absolute vorticity gradient. Consequently, the advances in understanding derived primarily from barotropic reasoning from many studies in the last five years represent an important contribution to the science.

### c. Full-physics baroclinic models

Professor T. N. Krishnamurti's group at Florida State University has used a high-resolution global spectral model to study various aspects of tropical cyclones. Sensitivity studies to soil moisture (Dastoor and Krishnamurti 1991) and radiative (Krishnamurti et al. 1991a) parameterizations have been made. Krishnamurti and Oosterhof (1989) have simulated the life cycle of Supertyphoon Hope during 1979 with the model. This study, and



other individual case studies (e.g., Heckley et al. 1987; Tuleya 1988), suggest the possibility of longer range track prediction under certain conditions.

As indicated above, the diagnosis of the effects contributing to tropical cyclone motion in these full-physics baroclinic models is difficult because of the many factors involved. However, the great advantage is the complete horizontal, vertical and time resolution in the model output compared to the data coverage in real storms. Krishnamurti et al. (1991b) have examined residue-free budgets (consistent with the model formulation) of the vorticity and divergence to gain insight into the recurvature dynamics. Using the simulation of Typhoon Colleen during 1989, they show that the leading term in the vorticity budget is the vorticity advection, with a smaller contribution from the beta term and the divergence term. They also conclude that advection of divergence by the divergent wind component in the front sector has a major contribution during the recurvature of Colleen. In comparison with a barotropic model, the full physics of the baroclinic model provides better forecasts of the tropical cyclone structure and of the intensities and positions of adjacent features such as the subtropical high cells that govern longer-range tracks.

Additional confirmation of the above results and interpretations are expected to be derived from the final TCM-90 data set, and from modeling studies based on the final analysis set. Given the importance of tropical cyclone structure in the motion problem, the next scientific challenge will then be to



understand what produces particular structures and causes structural changes.

**Acknowledgements.** The long-term support of the Office of Naval Research Marine Meteorology Program and of the Direct Research Fund of the Naval Postgraduate School is acknowledged. Colleagues who have shared their unpublished manuscripts are thanked. Professor Robert Haney provided constructive comments on the manuscript, which was skillfully prepared by Mrs. Penny Jones.



## REFERENCES

- Adem, J., 1956: A series solution for the barotropic vorticity equation and its application in the study of atmospheric vortices. *Tellus*, **8**, 364-372.
- Anthes, R. A., and J. E. Hoke, 1975: The effect of horizontal divergence and the latitudinal variation of the Coriolis parameter of the drift of a model hurricane. *Mon. Wea. Rev.*, **103**, 757-763.
- Carr, L. E., III, 1989: Barotropic vortex adjustment to asymmetric forcing with application to tropical cyclones. Ph.D. dissertation, Naval Postgraduate School, Monterey, CA 93943, 143 pp.
- Carr, L. E., III, and R. T. Williams, 1989: Barotropic vortex stability to perturbations from axisymmetry. *J. Atmos. Sci.*, **46**, 3177-3196.
- Carr, L. E., III, and R. L. Elsberry, 1990: Observational evidence for predictions of tropical cyclone propagation relative to steering. *J. Atmos. Sci.*, **47**, 542-546.
- Carr, L. E., III, and R. L. Elsberry, 1991: Analytical tropical cyclone asymmetric circulation for barotropic model initial conditions. *Mon. Wea. Rev.*, (accepted).
- Chan, J. C.-L., 1984: An observational study of the physical processes responsible for tropical cyclone motion. *J. Atmos. Sci.*, **41**, 1036-1048.
- Chan, J. C.-L., 1985: Identification of the steering flow for tropical cyclone motion from objectively analyzed wind fields. *Mon. Wea. Rev.*, **113**, 106-116.
- Chan, J. C.-L., and W. M. Gray, 1982: Tropical cyclone movement and surrounding flow relationships. *Mon. Wea. Rev.*, **110**, 1354-1374.
- Chan, J. C.-L., and R. T. Williams, 1987: Analytical and numerical studies of the beta-effect in tropical cyclone motion. Part I: Zero mean flow. *J. Atmos. Sci.*, **44**, 1257-1264.
- Chang, S. W., 1983: A numerical study of the interactions between two tropical cyclones. *Mon. Wea. Rev.*, **111**, 1806-1817.
- Dastoor, A., and T. N. Krishnamurti, 1991: The landfall and structure of a tropical cyclone: The sensitivity of model predictions to soil moisture parameterizations. *Boundary Layer Meteorology*, **55**, 345-380.

- DeMaria, M., 1985: Tropical cyclone motion in a nondivergent barotropic model. *Mon. Wea. Rev.*, **113**, 1199-1210.
- DeMaria, M., and J. C.-L. Chan, 1984: Comments on "A Numerical Study of the Interactions between Two Tropical Cyclones". *Mon. Wea. Rev.*, **112**, 1643-1645.
- Dong, K., 1988: On the relationship between tropical cyclone motion and intensity. *Mon. Wea. Rev.*, **116**, 964-968.
- Dong, K., and C. J. Neumann, 1986: The relationship between tropical cyclone motion and environmental geostrophic flows. *Mon. Wea. Rev.*, **114**, 115-122.
- Elsberry, R. L., 1986: Some issues related to the theory of tropical cyclone motion. Technical Report NPS 63-86-005, Naval Postgraduate School, Monterey, CA 93943, 23 pp.
- Elsberry, R. L., 1987a: Potential observing systems for tropical cyclone motion studies. Technical Report NPS 63-88-003, Naval Postgraduate School, Monterey, CA 93943, 47 pp.
- Elsberry, R. L., 1987b: Interim review of the possibilities and opportunities for the Office of Naval Research Tropical Cyclone Motion Research Initiative. Technical Report NPS 63-87-007, Naval Postgraduate School, Monterey, CA 93943, 31 pp.
- Elsberry, R. L., 1988a: ONR Tropical Cyclone Motion Research Initiative: First-year review, discussion and tentative hypotheses. Technical Report NPS 63-88-003, Naval Postgraduate School, Monterey, CA 93943, 86 pp.
- Elsberry, R. L., 1988b: ONR Tropical Cyclone Motion Research Initiative: Mid-year review, discussion and working group reports. Technical Report NPS-63-88-005, Naval Postgraduate School, Monterey, CA 93943, 103 pp.
- Elsberry, R. L., 1989a: ONR Tropical Cyclone Motion Research Initiative: Field Experiment Planning Workshop. Technical Report NPS 63-89-002, Naval Postgraduate School, Monterey, CA 93943, 79 pp.
- Elsberry, R. L., 1989b: ONR Tropical Cyclone Motion Research Initiative: Data assimilation considerations for field experiment analysis. Technical Report NPS 63-89-006, Naval Postgraduate School, Monterey, CA 93943, 64 pp.
- Elsberry, R. L., 1989c: ONR Tropical Cyclone Motion Research Initiative: Update on field experiment planning. Technical Report NPS-63-90-002, Naval Postgraduate School, Monterey, CA 93943, 64 pp.



- Elsberry, R. L., 1990: International experiments to study tropical cyclones in the western North Pacific. *Bull. Amer. Meteor. Soc.*, **71**, 1305-1316.
- Elsberry, R. L., W. M. Frank, G. J. Holland, J. D. Jarrell, R. L. Southern, 1987: A Global View of Tropical Cyclones. Office of Naval Research, Arlington, VA 22217, 185 pp.
- Elsberry, R. L., B. C. Diehl, J. C.-L. Chan, P. A. Harr, G. J. Holland, M. Lander, T. Neta, and D. Thon, 1990: ONR Tropical Cyclone Motion Initiative: Field experiment summary. Technical Report NPS-MR-91-001, Naval Postgraduate School, Monterey, CA 93943, 106 pp.
- Elsberry, R. L., and R. F. Abbey, Jr., 1991: Overview of the Tropical Cyclone Motion (TCM-90) field experiment. Preprints of 19th Conference on Hurricanes and Tropical Meteorology, American Meteor. Soc., Boston, MA 02108, 1-6.
- Evans, J. L., G. J. Holland and R. L. Elsberry, 1991: Interactions between a barotropic vortex and an idealized subtropical ridge. I. Vortex motion. *J. Atmos. Sci.*, **48**, 301-314.
- Feuer, S. E., and J. L. Franklin, 1991: Nested analysis of hurricane Gloria from dropwindsonde and Doppler radar data. Preprints of 19th Conference on Hurricanes and Tropical Meteorology, Amer. Meteor. Soc., Boston, MA 02108, 130-133.
- Fiorino, M., 1987: The role of vortex structure on tropical cyclone motion. Ph.D. dissertation, Naval Postgraduate School, Monterey, CA 93943, 369 pp.
- Fiorino, M., and R. L. Elsberry, 1989a: Some aspects of vortex structure in tropical cyclone motion. *J. Atmos. Sci.*, **46**, 979-990.
- Fiorino, M., and R. L. Elsberry, 1989b: Contributions of tropical cyclone motion by small, medium and large scales in the initial vortex. *Mon. Wea. Rev.*, **117**, 721-727.
- Flatau, M., 1991: The role of baroclinic processes in tropical cyclone motion. Preprints of 19th Conference on Hurricanes and Tropical Meteorology, Amer. Meteor. Soc., Boston, MA 02108, 349-352.
- Flierl, G. R., 1983: The physical significance of modons: Laboratory experiments and general integral constraints. *Dyn. Atmos. Oceans*, **7**, 233-266.
- Ford, D. M., R. L. Elsberry, P. A. Harr and P. H. Dobos, 1991: Forecasting tropical cyclone recurvature using an empirical orthogonal function representation of vorticity fields. Submitted to *Mon. Wea. Rev.*

- Franklin, J. L., 1990: Dropwindsonde observations of the environmental flow of hurricane Josephine (1984): Relationships to vortex motion. *Mon. Wea. Rev.*, **118**, 2732-2744.
- Fujiwhara, S., 1923: On the growth and decay of vortical systems. *Quart. J. Roy. Meteor. Soc.*, **49**, 75-104.
- George, J. E., and W. M. Gray, 1976: Tropical cyclone recurvature and nonrecurvature as related to surrounding wind-height fields. *J. Appld. Meteor.*, **16**, 34-42.
- Gray, W. M., 1989: Summary of ONR sponsored tropical cyclone motion research and future plans. Appendix D of Technical Report NPS 63-89-002, Naval Postgraduate School (R. L. Elsberry, Ed.), Monterey, CA 93943, 68-79.
- Gray, W. M., 1991: Tropical cyclone propagation. Preprints of 19th Conference on Hurricanes and Tropical Meteorology, Amer. Meteor. Soc., Boston, MA 02108, 385-390.
- Gross, J. M., 1991: The effect of shallow, medium and deep layer mean wind in the beta and advection model. Preprints of 19th Conference on Hurricanes and Tropical Meteorology, Amer. Meteor. Soc., Boston, MA 02108, 104-106.
- Harr, P. A., and R. L. Elsberry, 1991: Tropical cyclone track characteristics as a function of large-scale circulation anomalies. *Mon. Wea. Rev.*, **119**, 1448-1468.
- Harr, P. A., T. Neta and R. L. Elsberry, 1991: ONR Tropical Cyclone Motion Research Initiative: Data users guide to observations. Technical Report NPS-MR-91-002, Naval Postgraduate School, Monterey, CA 93943, 123 pp.
- Heckley, W. A., M. J. Miller and A. K. Betts, 1987: An example of hurricane tracking and forecasting with a global analysis-forecasting system. *Bull. Amer. Meteor. Soc.*, **68**, 226-229.
- Hodanish, S. J., 1991: An observational analysis of tropical cyclone recurvature. Atmos. Sci. paper 480, Colo. State Univ., Ft. Collins, CO 80523, 124 pp.
- Holland, G. J., 1983: Tropical cyclone motion: Environmental interaction plus a beta effect. *J. Atmos. Sci.*, **40**, 328-342.
- Holland, G. J., 1984: Tropical cyclone motion: A comparison of theory and observation. *J. Atmos. Sci.*, **41**, 68-75.
- Holland, G. J., 1991: On the meandering nature of tropical cyclone tracks. Preprints of 19th Conference on Hurricanes and Tropical Meteorology, Amer. Meteor. Soc., Boston, MA 02108, 53-55.

- Holland, G. J., and G. S. Dietachmayer, 1991: On the interaction of tropical-cyclone scale vortices. III: Continuous barotropic vortices. *Quart. J. Roy. Meteor. Soc.*, submitted..
- Holland, G. J., and J. L. Evans, 1991: Interactions between a barotropic vortex and an idealized subtropical ridge. II. Structure changes. *J. Atmos. Sci.* (accepted).
- Holland, G. J., and M. Lander, 1991: On the meandering nature of tropical cyclones. *J. Atmos. Sci.* (submitted).
- Holland, G. J., L. M. Leslie and B. Diehl, 1991: Comments on "The Detection of Flow Asymmetries in the Tropical Cyclone Environment." *Mon. Wea. Rev.*, (submitted).
- Kaplan, J., and J. L. Franklin, 1991: The relationship between the motion of tropical storm Florence (1988) and its environmental flow. Preprints of 19th Conference on Hurricanes and Tropical Meteorology, Amer. Meteor. Soc., Boston, MA 02108, 93-97.
- Kasahara, A., and G. W. Platzman, 1963: Interaction of a hurricane with the steering flow and its effect upon hurricane trajectory. *Tellus*, 15, 321-335.
- Keenan, T. D., 1982: A diagnostic study of tropical cyclone forecasting in Australia. *Aust. Meteor. Mag.*, 30, 69-80.
- Khandekar, M. L., and G. V. Rao, 1971: The mutual interaction of multiple vectors and its influence on binary and single tropical vortex storms. *Mon. Wea. Rev.*, 99, 840-846.
- Krishnamurti, T. N., and D. Oosterhof, 1989: Prediction of the life cycle of a super typhoon with a high resolution global model. *Bull. Amer. Meteor. Soc.*, 70, 1218-1230.
- Krishnamurti, T. N., K. S. Yap and D. Oosterhof, 1991a: Sensitivity of tropical storm forecast to radiative destabilization. *Mon. Wea. Rev.*, 119, 2176-2205.
- Krishnamurti, T. N., 1991: Typhoon prediction with a high resolution model. Preprints, International Conference on Mesoscale Meteor. and TAMEX. Meteor. Soc. Rep. of China, Taipei, Taiwan, Republic of China.
- Lander, M., and G. J. Holland, 1991: On the interaction of tropical-cyclone scale vortices: Part I: Observations. Submitted to *Quart. J. Roy. Meteor. Soc.*
- Li, Tianming, and Yongti Zhu, 1991: Numerical experiment on the effect of environmental flows on tropical cyclone motion. *Acta Meteorologica Sinica*, 5, 111-117.



- Lord, S. J., 1989: Vorticity advection from nested analyses of the hurricane environment. Extended abstracts, 18th Conference on Hurricanes and Tropical Meteorology, San Diego, Amer. Meteor. Soc., 202-203.
- Lord, S. J., and J. L. Franklin, 1987: The environment of Hurricane Debby (1982). Part I: Winds. *Mon. Wea. Rev.*, **115**, 2760-2780.
- Madala, R. V., and S. A. Piacsek, 1975: Numerical simulation of asymmetric hurricanes on a beta-plane with vertical shear. *Tellus*, **27**, 453-468.
- Marks, F. D., Jr., R. A. Houze, Jr. and J. F. Gamache, 1991: Dual-aircraft investigation of the inner core of Hurricane Norbert. Part I. Kinematic structure. Submitted to *J. Atmos. Sci.*
- Mathur, M. B., 1991: The National Meteorological Center's Quasi-Lagrangian Model for hurricane prediction. *Mon. Wea. Rev.*, **119**, 1419-1447.
- Neumann, C. J., 1979: On the use of deep-layer-mean geopotential height fields in statistical prediction of tropical cyclone motion. 6th Conference on Prob. and Stat. in Atmos. Sci., Amer. Meteor. Soc., Boston, MA 02108, 32-38.
- Peng, M. S., and R. T. Williams, 1990: Dynamics of vortex asymmetries and their influence on vortex motion on a beta-plane. *J. Atmos. Sci.*, **47**, 1987-2003.
- Peng, M. S., and R. T. Williams, 1991: Stability analyses of barotropic vortices. *Geophys. Astrophys. Dyn.*, **58**, 263-283.
- Reeder, M. J., R. K. Smith, and S. J. Lord, 1991: The detection of flow asymmetries in the tropical cyclone environment. *Mon. Wea. Rev.*, **119**, 848-854.
- Ritchie, E. A., and G. J. Holland, 1991: On the interaction of tropical-cyclone scale vortices. II. Discrete vortex patches. *Quart. J. Roy. Meteor. Soc.*, submitted.
- Rossby, C.-G., 1948: On the displacements and intensity changes of atmospheric vortices. *J. Mar. Res.*, **7**, 175-196.
- Roux, F., and F. D. Marks, Jr., 1991: Eyewall evolution in hurricane Hugo deduced from successive airborne Doppler observations. Preprints of 19th Conference on Hurricanes and Tropical Meteorology, Amer. Meteor. Soc., Boston, MA 02108, 558-563.
- Shapiro, L. J., 1983: The asymmetric boundary layer flow under a translating hurricane. *J. Atmos. Sci.*, **40**, 1984-1998.



- Shapiro, L. J., 1991: Hurricane vortex motion and evolution in a three-layer model. Submitted to *J. Atmos. Sci.*
- Shapiro, L. J., and K. V. Ooyama, 1990: Barotropic vortex evolution on a beta plane. *J. Atmos. Sci.*, **47**, 170-187.
- Smith, R. K., 1991: An analytic theory of tropical cyclone motion in a barotropic shear flow. Submitted to *Quart. J. Roy. Meteor. Soc.*
- Smith, R. K., and W. Ulrich, 1990: An analytical theory of tropical cyclone motion using a barotropic model. *J. Atmos. Sci.*, **47**, 1973-1986.
- Smith, R. K., and W. Ulrich, 1991: Vortex motion in relation to the absolute vorticity gradient of the vortex environment. Submitted to *J. Atmos. Sci.*
- Smith, R. K., W. Ulrich and G. Dietachmayer, 1990: A numerical study of tropical cyclone motion using a barotropic model. Part I: The role of vortex asymmetries. *Quart. J. Roy. Meteor. Soc.*, **116**, 337-362.
- Sutyryn, G. G., 1987: The beta effect and the evolution of a localized vortex. *Sov. Phys. Dokl.*, **32**, 791-793.
- Sutyryn, G. G., 1988: Motion of an intense vortex on a rotating globe. *Izv. Akad. Nauk SSSR, Mekh. Zhidk. Gaza*, 215-223.
- Sutyryn, G. G., 1989: Forecast of intense vortex motion with an azimuthal modes model. *Mesoscale/Synoptic Coherent Structures in Geophysical Turbulence*, J. C. J. Nihoul and B. M. Jamart, Eds., Elsevier Oceanography Series, No. 50, Elsevier, Amsterdam, pp. 771-782.
- Talbert, K. M., 1987: The effect of vertical wind shear on tropical cyclone movement. Masters Thesis, Department of Atmospheric Sciences, North Carolina State University. Available from NTIS, Accession No. ADA-197-218.
- Tuleya, R. E., 1988: A numerical study of the genesis of tropical storms observed during the FGGE year. *Mon. Wea. Rev.*, **116**, 1188-1208.
- Ulrich, W., and R. K. Smith, 1991: A numerical study of tropical cyclone motion using a barotropic model. II. Motion in spatially-varying large-scale flows. *Quart. J. Roy. Meteor. Soc.*, **117**, 107-124.
- Velden, C. S., and L. M. Leslie, 1991: The basic relationship between tropical cyclone intensity and the depth of the environmental steering layer in the Australian region. *Wea. and Fcst.*, **6**, 244-253.

- Wang, B. and Li, 1991: Numerical study of the beta-drift of three dimensional vortices. Preprints, 19th Conference on Hurricanes and Tropical Meteorology, American Meteor. Soc., Boston, MA, 02108, 358-361.
- Weber, H. C., 1991: The stability of barotropic vortices. Preprints, 19th Conference on Hurricanes and Tropical Meteorology, American Meteor. Soc., Boston, MA, 02108, 381-382.
- Williams, R. T., and J. C.-L. Chan, 1991: Numerical and analytical studies of the beta-effect in tropical cyclone motion. Part II. East-west mean flow. To be submitted.
- Willoughby, H. E., 1979: Forced secondary circulation in hurricanes. *J. Geophys. Res.*, **84**, 3173-3183.
- Willoughby, H. E., 1988: Linear motion of a shallow-water barotropic vortex. *J. Atmos. Sci.*, **45**, 1906-1928.
- Willoughby, H. E., 1990: Linear normal modes of a moving, shallow-water barotropic vortex. *J. Atmos. Sci.*, **47**, 2141-2148.
- Willoughby, H. E., 1991: Linear motion of a shallow-water barotropic vortex as an initial value problem. Submitted to *J. Atmos. Sci.*
- Wu, C.-C., and K. A. Emanuel, 1991: The effect of ambient vertical shear on tropical cyclone motion. Preprints, 19th Conference on Hurricanes and Tropical Meteorology, American Meteor. Soc., Boston, MA 02108, 353-355.

## Distribution List

Office of Naval Research (Code 1122MM) 800 N. Quincy Street Arlington, VA 22217-5000	1
Dr. Robert L. Haney (Code MR/Hy) Chairman, Department of Meteorology Naval Postgraduate School Monterey, CA 93943-5000	1
Dr. Russell L. Elsberry (Code MR/Es) Department of Meteorology Naval Postgraduate School Monterey, CA 93943-5000	193
Library (Code 0142) Naval Postgraduate School Monterey, CA 93943-5000	2
Dean of Research (Code 08) Naval Postgraduate School Monterey, CA 93943-5000	1
Defense Technical Information Center Cameron Station Alexandria, VA 22304-6145	2







DUDLEY KNOX LIBRARY



3 2768 00337485 1